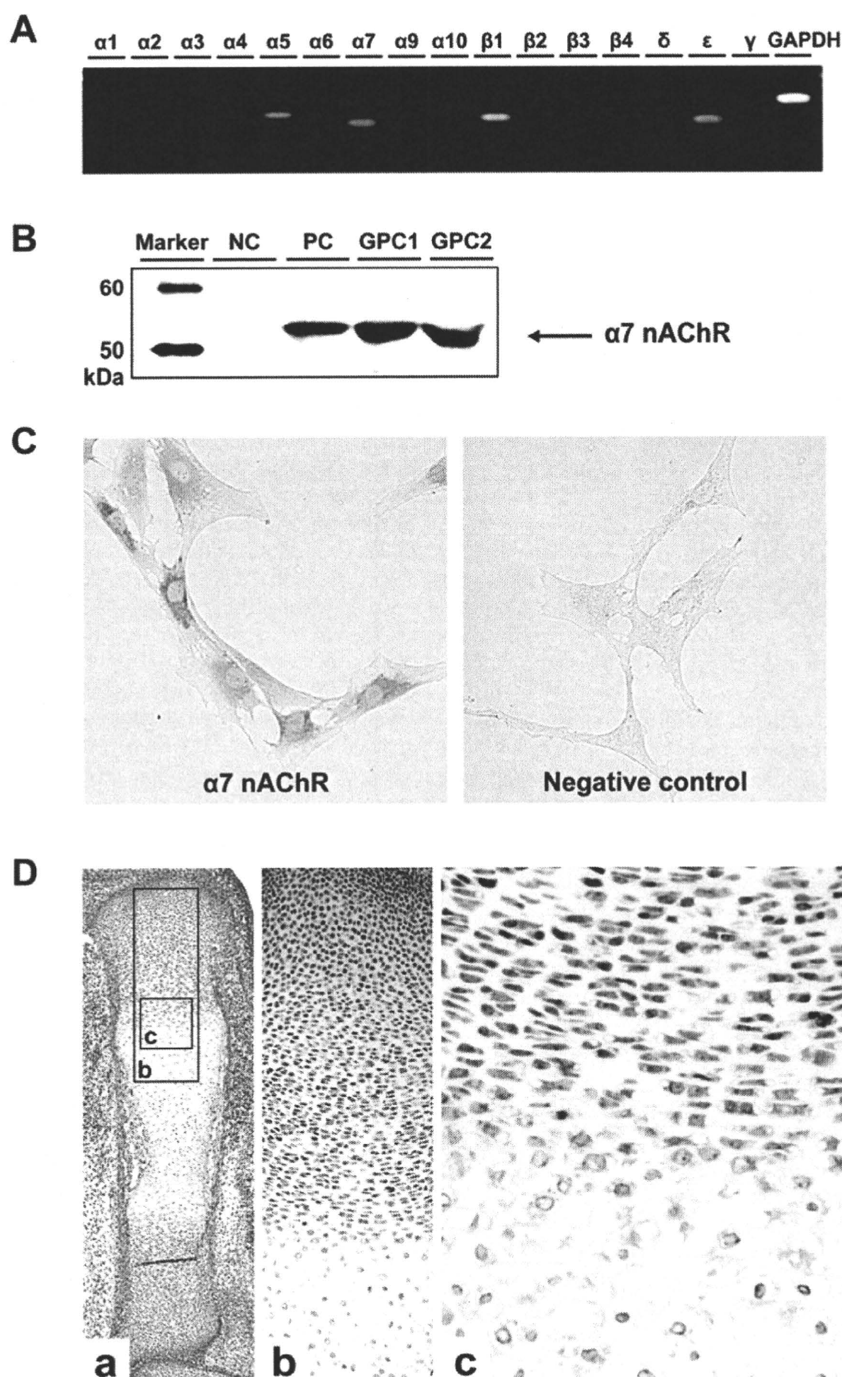

Figure 1. Detection and localization of nAChR subunits in growth plate chondrocytes. A: The expression of each subunit of nAChR. Total RNA was isolated from primary culture of human growth plate chondrocytes. The primers for each subunit are listed in Tables S1–S3. RT-PCR amplified products of alpha5, alpha7, beta1 and epsilon subunits of nAChR and GAPDH. B: Western blot analysis of alpha7 subunit of nAChR in primary chondrocyte cultures. NC: negative control (adipocyte), PC: positive control (PC-12 cell), GPC1,2: human growth plate chondrocyte derived from extra fingers of two individuals. C: Immunocytochemical analysis of alpha7 nAChR subunit in human growth plate chondrocytes. Primary chondrocytes were stained with alpha7 nAChR subunit-specific antibody. D: Immunohistochemical analysis of alpha7 nAChR subunit in tibia of E15.5 fetuses. Alpha7 nAChR are detected at resting, proliferating and pre-hypertrophic chondrocytes of murine growth plate.
doi:10.1371/journal.pone.0003945.g001

of maternal nicotine exposure on skeletal development of murine fetuses in which the alpha7 nAChR gene is disrupted. Maternal genotype is alpha7 nAChR +/− in this experiment (Figure 6), unlike the experiment using wild type mice (Figure 5, maternal genotype: alpha7 nAChR +/+), and littermate fetuses (alpha7 nAChR −/− and alpha7 nAChR +/+) were compared to exclude the effect of nicotine on maternal bodies. Nicotine significantly reduced FL and HL/FL in alpha7 nAChR +/+ fetuses but not in alpha7 nAChR −/− fetuses (Figure 6A, B). However, nicotine did not significantly affect body weight (BW) in both genotypes

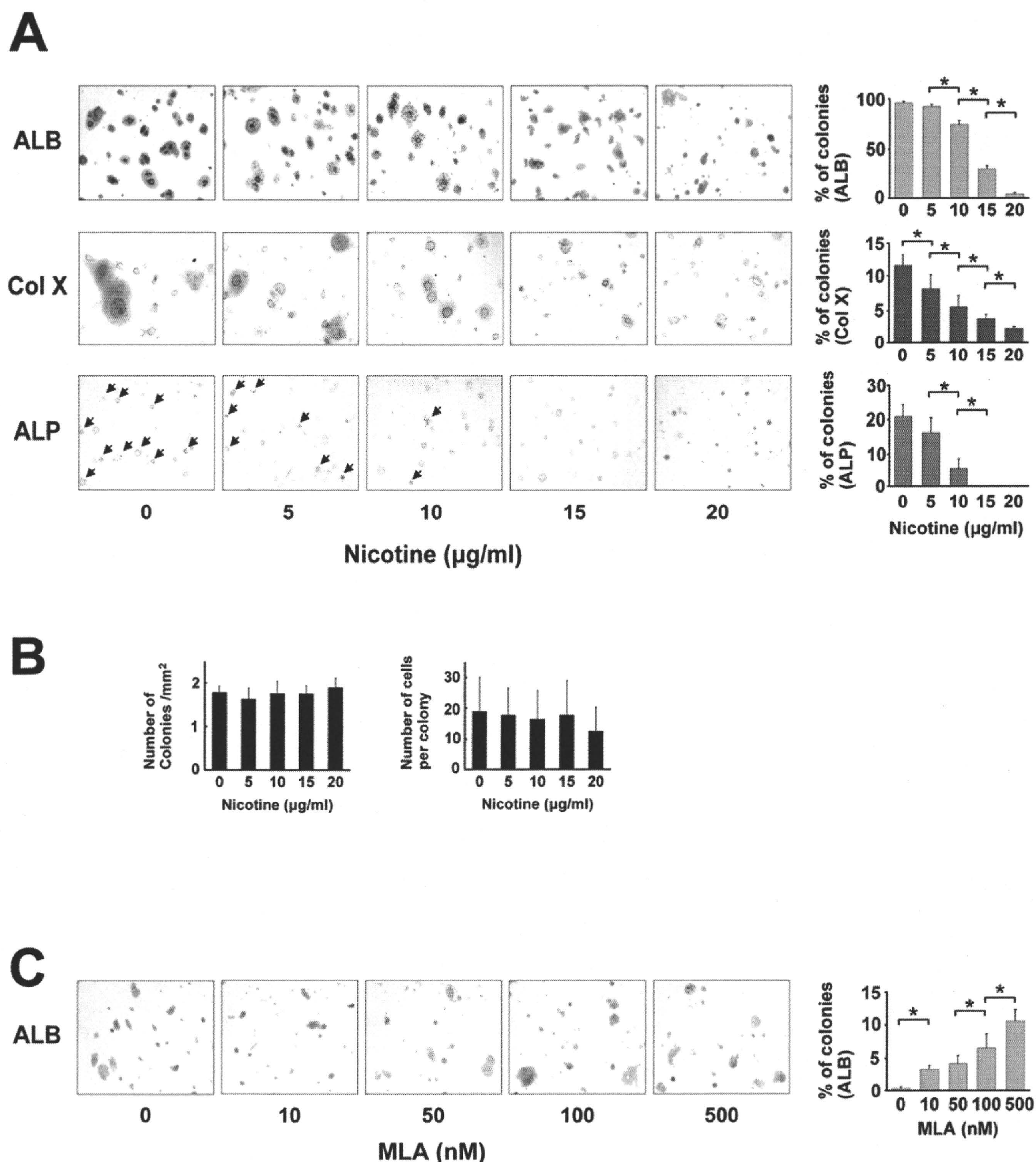

Figure 2. Effect of nicotine on growth plate chondrocytes in agarose gel. Growth plate chondrocytes were cultured in an agarose gel using the modified method previously described [28], and exposed to nicotine and MLA, a specific antagonist for alpha7 nAChR, at the indicated concentration. After three weeks of cultivation, suspension agarose was transferred to a glass slide and the following histological analyses were then performed. A: Microscopic appearance of chondrocyte colonies. From top to bottom: ALB (Alcian blue stain), Col X (immunocytochemistry by an anti-Col X antibody), ALP (enzyme cytochemistry of alkaline phosphatase). For ALB and Col X stain, the slides were counterstained with kernechtrot and hematoxylin, respectively. Percentage of ALB- stained, Col X- positive, and Alkaline phosphatase- positive colonies were counted (right panel, from top to bottom). All the ALP positive colonies in the panels are indicated by arrowheads. Nicotine concentration-dependently suppressed the percentage of the colonies stained with ALB, Col X, and ALP. *, statistically significant, $P<0.02$. B: Number of colonies and number of cells per colony. The number of colonies with a diameter greater than 50 μm (left panel) and cell number per colony (right panel) were counted on the ALB- stained agarose gel slides. C: Microscopic appearance of chondrocyte colonies stained with ALB. MLA reversed the decrease of ALB- positive matrix in a concentration-dependent manner under constant nicotine concentration (20 μg/ml). The percentage of ALB-positive colonies exceeded 10% by using 500 nM MLA. *, statistically significant, $P<0.02$.

doi:10.1371/journal.pone.0003945.g002

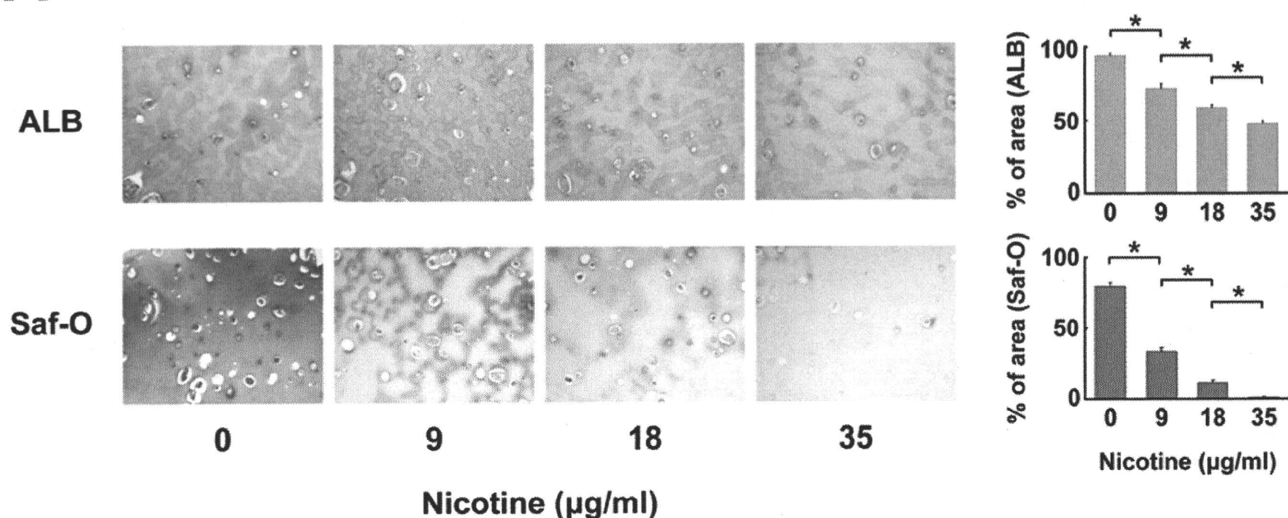

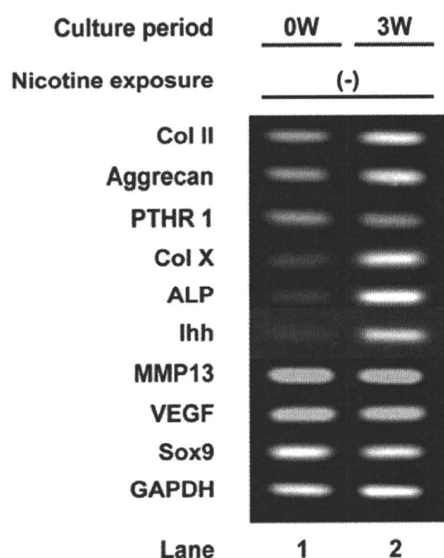

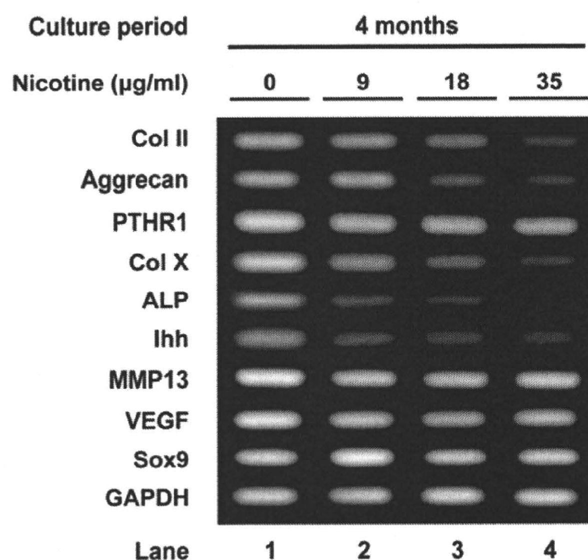

Figure 3. Long-term (four months) effect of nicotine on growth plate chondrocytes in alginate beads. Growth plate chondrocytes in alginate beads were exposed to the indicated concentration of nicotine for four months. A: Microscopic view of chondrocytes in alginate beads after four-months cultivation. Upper panels: ALB stain, lower panels: Safranin-O stain. Chondrocytes were surrounded by matrix which they secreted. Nicotine decreased the area stained with ALB or Safranin-O in a concentration-dependent manner. *, statistically significant, $P<0.02$. B: RT-PCR analysis of chondrocyte-specific gene expression in the chondrocytes at the start of cultivation (lane 1: 0W) and three weeks (lane 2: 3W). From top to bottom: genes for Col II, Aggrecan, parathyroid hormone receptor type 1 (PTHR1), Col X, alkaline phosphatase (ALP), Indian hedgehog (Ihh), matrix metalloproteinase type13 (MMP13), vascular endothelial growth factor (VEGF), Sox9 and GAPDH. C: RT-PCR analysis of chondrocyte-specific gene expression in chondrocytes embedded in alginate beads exposed to the indicated concentration of nicotine for four months. Expression of early stage matrix-gene (Col II and Aggrecan) and markers of hypertrophic chondrocytes (Col X, ALP and Ihh) increased after three weeks of cultivation (B). Nicotine decreased the expression of these genes in a concentration-dependent manner, but had little effect for the expression of MMP13, VEGF, and control genes (Sox9 and GAPDH) (C).
doi:10.1371/journal.pone.0003945.g003

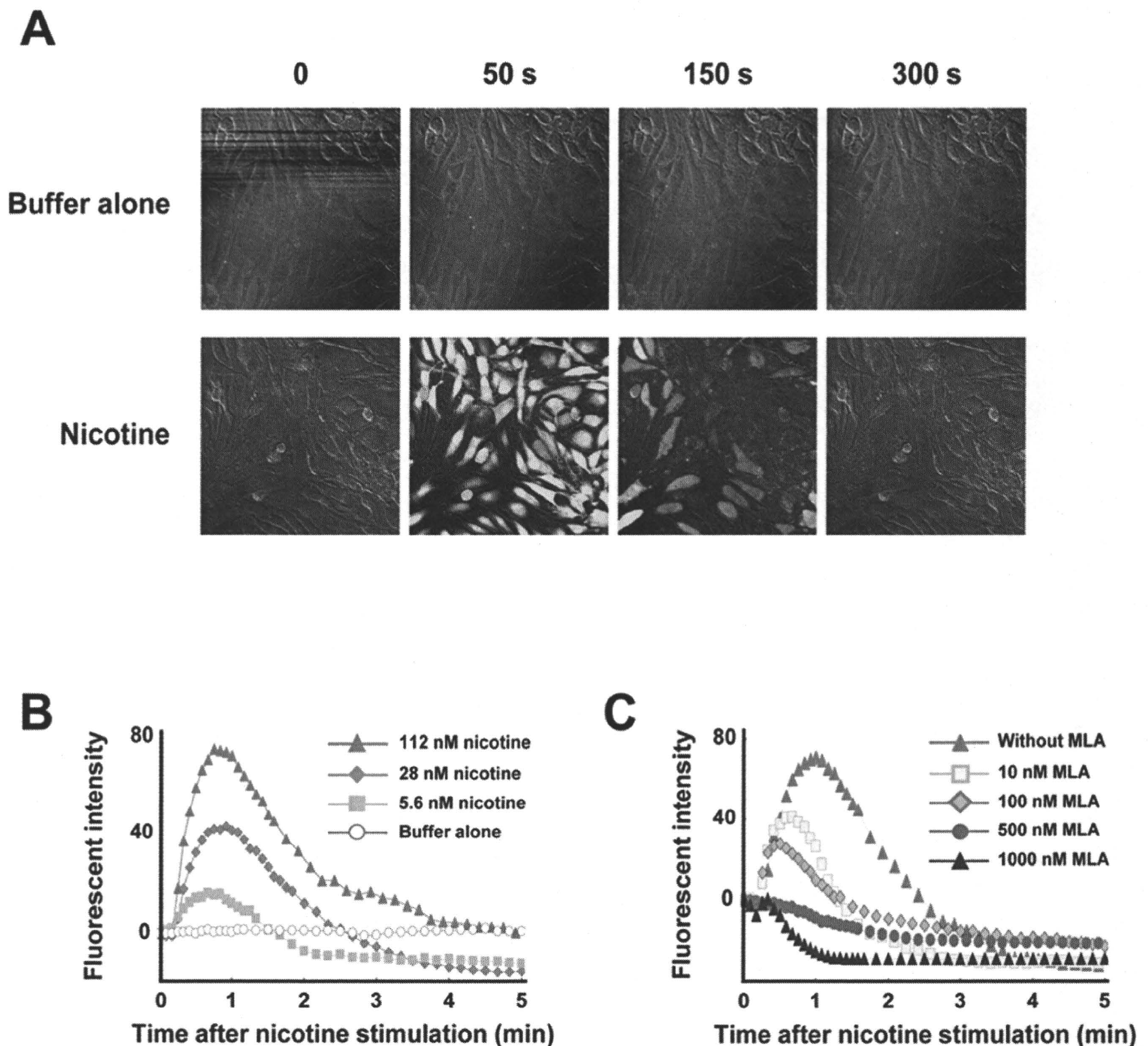

Figure 4. Calcium influx assay in primary chondrocyte culture. Nicotine-stimulated calcium signaling was investigated by the use of a fluorescent Ca^{2+} indicator. Primary chondrocyte cultures were stimulated by nicotine with or without MLA, the specific antagonist of alpha7 homomeric nAChR. A: Addition of assay buffer alone elicits no reaction (upper panels: negative control). Nicotine elicits a transient increase of intra-cellular calcium (lower panels). B: Nicotine elicits a transient increase of intra-cellular calcium in a concentration-dependent manner. C: MLA inhibits nicotine-induced calcium influx in a concentration-dependent manner. The cells were treated with MLA 30 min before nicotine stimulation.
doi:10.1371/journal.pone.0003945.g004

(Figure 6C). Besides, scatterplot and correlation between the FL and the BW revealed that nicotine downwardly shifted the linear slope in alpha7 nAChR +/+ fetuses but had no effect in alpha7 nAChR −/− fetuses (Figure 6D). These findings suggest that maternal nicotine exposure decreased the fetal endochondral ossification through the fetal alpha7 nAChR in vivo.

Discussion

Alpha7 nAChR was originally identified as a subunit of neuronal nAChR, and has also been shown to be functional in both neuronal and non-neuronal, i.e., non-excitable cells such as lymphocytes, vascular endothelial cells, keratinocytes and bronchial epithelium [16]. In this study, we demonstrated the expression of the alpha7 subunit of nAChR at resting to pre-hypertrophic chondrocytes in murine growth plate and on a culture of human growth plate chondrocytes, and the involvement of alpha7 nAChR in nicotine-induced delayed skeletal growth. The novel findings of alpha7 nAChR in chondrocytes suggest that the effect of smoking on delayed skeletal growth is directly correlated with nicotinic action on chondrocytes.

Direct effect of nicotine on human growth plate chondrocytes

Maternal nicotine exposure decreases the width of the hypertrophic zone of growth plate, increases apoptotic chondrocytes, and reduces the length of femur in rat [20]. Contrarily, nicotine has been shown to up-regulate glycosaminoglycan and

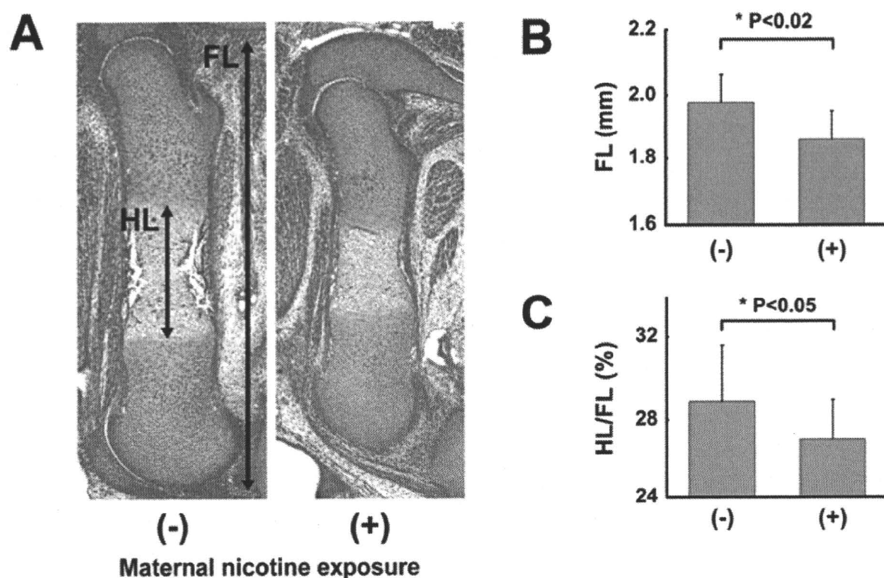

Figure 5. Maternal nicotine exposure in wild-type mice. Ovulation-induced pregnant mice were mated and were given drinking water with nicotine during pregnancy. At noon on gestational day 15, the fetuses were sacrificed, and their legs were histologically investigated. A: Skeletal growth estimated by measuring the femur length (FL) and the length of the hypertrophic zone of the femur (HL). B: FL (mm), C: HL/FL (%) of E15.5 fetuses whose mothers were given drinking water with or without nicotine. Nicotine significantly decreased FL and HL/FL.
doi:10.1371/journal.pone.0003945.g005

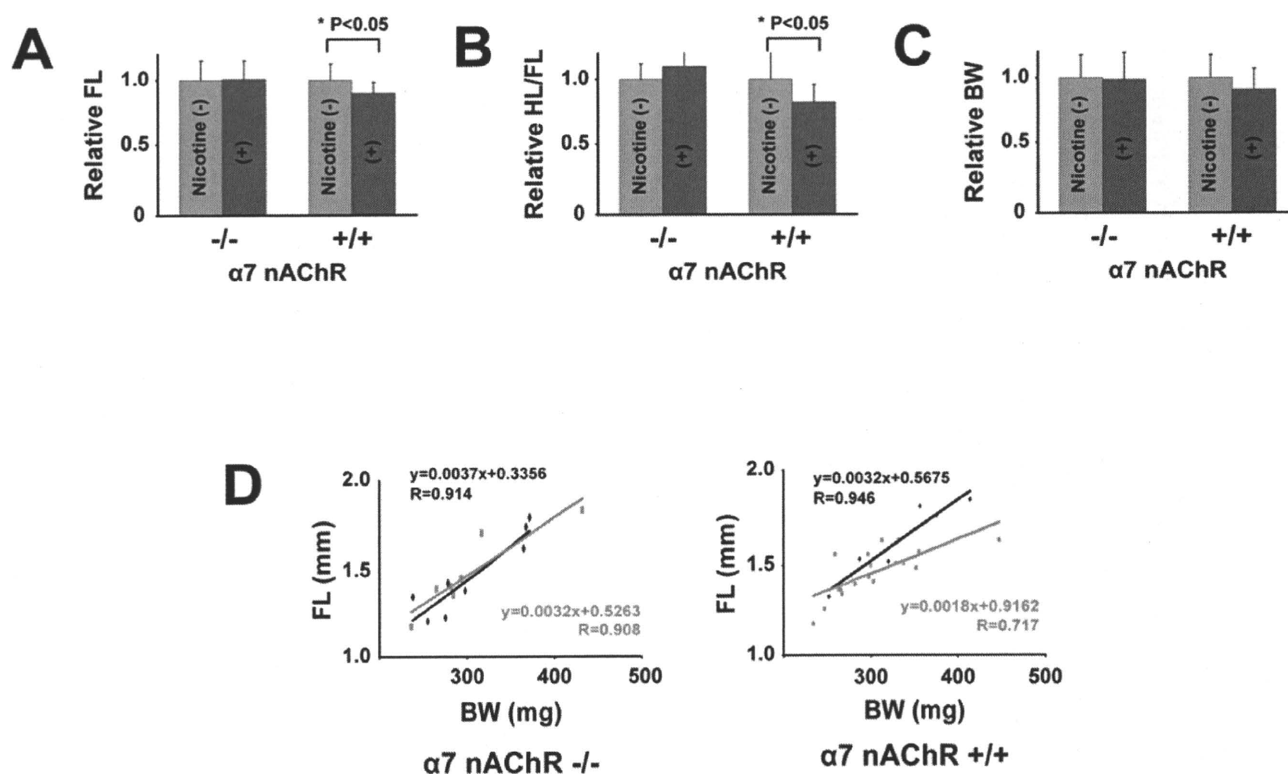

Figure 6. Maternal nicotine exposure in alpha7 nAChR-disrupted mice. A–C: FL, HL/FL, and body weight (BW) of alpha7 nAChR −/− and alpha7 nAChR +/+ E15.5 littermate fetuses. Alpha7 nAChR +/− female were mated with alpha7 nAChR +/− male, and given drinking water with or without nicotine during pregnancy. Relative FL, HL/FL, and BW were calculated, each value in mice that did not receive nicotine was regarded as equal to 1.0. Nicotine significantly reduced FL and HL/FL in alpha7 nAChR +/+ fetuses but not in alpha7 nAChR −/− fetuses (A,B). Nicotine did not significantly reduce BW in either genotype (C). D: Scatterplot and correlation between the FL and BW of mice with (red line) or without (black line) exposure to nicotine. In alpha7 nAChR +/+ fetus, Nicotine downwardly shifts the linear slope in alpha7 nAChR +/+ fetuses but not in alpha7 nAChR −/− fetuses.
doi:10.1371/journal.pone.0003945.g006

collagen synthesis of human articular chondrocytes in vitro [21]. Cultured human growth plate chondrocytes derived from infant fingers serve as a good model for analyzing whether nicotine has direct action on growth plate chondrocytes. The present findings of nicotinic effect, i.e. decreasing matrix synthesis and suppressing hypertrophic differentiation but not proliferation on growth plate chondrocytes in vitro, indicate the direct effect of nicotine on growth plate chondrocytes. The findings are consistent with reports that maternal nicotine exposure has a negative effect on endochondral ossification in animals [13]. Besides, these findings are consistent, considering the fact that longitudinal skeletal growth is partly caused by matrix synthesis and hypertrophic differentiation of chondrocytes. Confirmation of the animal model using "human" chondrocytes is essential since certain chemicals, such as thalidomide, exhibit different effects in humans and rodents.

Differences of expression levels of the genes for Col X, ALP, Ihh, MMP13, and VEGF in alginate beads culture (Figure 3B, C) may attribute to differential regulation among hypertrophic markers. Expression of the Ihh, Col X, and ALP genes were down-regulated by nicotine and the MMP13 and VEGF genes remained unaffected. Alternatively, the difference could be a result of chondrocyte culture, that is, artifactual induction ex vivo, and the MMP13 and VEGF genes were indeed expressed at the start of alginate bead culture with chondrocytes at passage 1 (Fig. 3B, lane 1: "0 W"). In contrast, the Col X, ALP, and Ihh genes were appropriately regulated after three-dimensional culture (Figure 3B, lane 2: "3 W"; Figure 3C, lane 1: without exposure to nicotine), as is the case with gene regulation in the growth plate.

Involvement of alpha7 nAChR in delayed endochondral ossification

The alpha7 nAChR-null mice exhibit normal development, including neural tissue, but alpha7 nAChR-null mice lack nicotinic currents in hippocampal neurons [22], and show abnormalities in late-stage keratinocyte development in the epidermis [23]. Lack of phenotypic abnormality in the femur of fetuses (Figure 5B) and adults indicates that ACh signaling through alpha7 nAChR has little involvement in the process of physiological skeletal growth. Results using MLA, the antagonist to alpha7 nAChR, strongly suggest the involvement of alpha7 nAChR in the nicotinic effect on chondrocytes. Such low-molecular weight substances may, however, have additional unclarified action in addition to any "specific" action. The proof of alpha7 nAChR involvement in delayed skeletal growth was strengthened by the in vivo experiments with alpha7 nAChR gene-disrupted mice. Especially so, considering the fact that maternal nicotine exposure caused delayed skeletal growth in only alpha7 nAChR +/+ fetuses compared with their alpha7 nAChR −/− littermates, fetal alpha7 nAChR but not maternal alpha7 nAChR is responsible for the mechanism of nicotine-induced delayed skeletal growth.

Since nicotine exposure has been reported to be epidemiologically and experimentally correlated with maternal effect, i.e., abnormal placental function and blood flow [10], the physiological and pathological function of alpha7 nAChR in growth plate was confirmed by comparing "littermates" of alpha7 nAChR (Figure 6B). This comparison confirms involvement of alpha7 nAChR on the fetus, and eliminates a possibility of maternal effect. Furthermore, decrease of relative femur length (Figure 6C, scatterplot and correlation, right panel, alpha7 nAChR +/+) and lack of nicotinic effect on body weight of alpha7 nAChR fetuses (Figure 6B, right panel, "BW") by maternal nicotine exposure indicate a specific effect of nicotine on bone growth rather than a systemic effect. Therefore, the effect of smoking during pregnancy on skeletal growth may be attributed to this direct action of nicotine on growth plate chondrocytes, at least in part.

Our studies suggest that, from the large number of chemicals associated with cigarette smoking, nicotine may cause delayed skeletal growth and, indeed, amniotic fluid and breast milk both have higher concentrations of nicotine than maternal serum does [24]. In addition, metabolism of nicotine in the fetus and child is much slower than that in adults [25]. We therefore should pay close attention to the effect of smoking, regardless of being active or passive, on growth plate chondrocytes. This nicotinic effect may also extend to the delay of fracture repair or generation of non-union in adults, since the process of bone repair also partly depends on endochondral ossification.

Materials and Methods

Chondrocyte cultures

Human chondrocytes were isolated from epiphysis of extra fingers, which were surgically excised from patients with polydactyly. Ethical approval for tissue collection was granted by the Institutional Review Board of the National Research Institute for Child Health and Development, Tokyo, Japan (#88). Minced tissue was incubated for 1 h at 37°C in 0.08% trypsin in PBS, then for 6 h at 37°C in 0.2% collagenase type 1 (Wako, Osaka, Japan) in Dulbecco's Modified Eagle's medium (DMEM). The released cells were washed and resuspended in DMEM containing 10% fetal bovine serum (FBS, Sanko Junyaku Co., Tokyo, Japan, lot number: 27110307) and plated at a density of 1×10^6 cells per 100 mm dish for primary monolayer cultures, or 1×10^6 cells per 35 mm dish for calcium influx assay and immunocytochemical assay of nAChR. In each experiment, we used one lot of cultured chondrocytes from extra fingers obtained from four patients.

RT-PCR for detection of nAChR subunit

Total RNA was prepared from epiphysis of extra fingers using Isogen (Nippon Gene) according to the manufacturer's recommendations. DNase-treated RNA was reverse transcribed in 20 µl of RT-PCR mix (50 mM Tris, pH 8.3, 3 mM $MgCl_2$, 75 mM KCl, 50 mM dNTPs, 2.5 µM oligo$(dT)_{20}$, 5 mM DTT, 2 U RNaseOUT and 10 U SuperScriptIII (Invitrogen) at 50°C for 1 h. The PCR was performed in a final volume of 50 µl containing 1 µl of the single strand cDNA product, 25 mM TAPS (pH 9.3), 50 mM KCl, 2.0 mM $MgCl_2$, 1 mM β-mercaptoethanol , 200 µM dNTPs, and AmpliTaq Gold (Applied Biosystems) and 20 pmol of each forward (5′) and reverse (3′) primers (Table S1). For each experiment the housekeeping gene GAPDH was amplified with 25–35 cycles to normalize the cDNA content of the samples. The amplification was performed for 30 cycles, with other conditions following polymerase-producing manufacturer's recommendations. Human brain and skeletal muscle RNAs were purchased from Ambion (Austin, TX).

Western blot analysis for detection of nAChR subunit

Total proteins were isolated from primary monolayer cultures using CelLyticTM-M Mammalian Cell Lysis/Extraction Reagent (Sigma). The proteins were separated by SDS-PAGE (Bio-Rad) in a 10% acrylamide gel, then blotted at 60 V for 2 h at 4°C onto a nitrocellulose membrane. Non-specific binding was blocked by incubation in TBS containing 10% BSA and 0.05% Tween-20. The membrane was subsequently incubated at 4°C overnight with the monoclonal antibody to nicotinic acetylcholine receptor, alpha7 subunit (Sigma, St-Louis, MO; product number: N 8158) diluted 1:3000. After rinsing, the membrane was incubated for 1 h at room temperature in horseradish peroxidase-conjugated rabbit

anti-rat IgG antibody (Sigma; A 5795) at a dilution of 1:3000 in TBS containing 0.05% Tween-20. After rinsing, the membrane was immersed in ECL solution (GE Healthcare, Buckinghamshire, UK). Then, the blots were visualized by LAS-1000plus IDX2, the luminescent image analyzer (Fuji Photo Film, Japan).

Immunocytochemical and immunohistochemical analysis

Immunocytochemical analysis was performed as previously described [26]. Briefly, dishes were incubated with antibody to alpha7 subunit of nAChR in PBS containing 1% BSA. As a methodological control, the primary antibody was omitted. After washing in PBS, dishes were incubated with horseradish peroxidase (HRP)-conjugated rabbit anti-rat IgG antibody. Staining was developed by using a solution containing diaminobenzidine and 0.01% H_2O_2 in 0.05 M Tris-HCl buffer, pH 6.7.

For immunohistochemical analysis, hind legs of E15.5 C57BL/6J mice were prepared, fixed in 4% paraformaldehyde phosphate buffer solution (Wako) overnight at 4°C, and embedded in paraffin. Immunohistochemical analysis was performed as previously described [27]. Briefly, slides were treated with 0.4% pepsin (DAKO) at 37°C for 30 min, incubated with primary antibody to alpha7 subunit of nAChR(Sigma, product number: N 8158) diluted 1:2000 in PBS containing 1% BSA at room temperature for 3 h, and incubated with simple mouse stain MAX-PO (RAT), a second antibody, at room temperature for 1 h. Staining was developed by using a solution containing diaminobenzidine and 0.01% H_2O_2 in 0.05 M Tris-HCl buffer, pH 6.7. Finally, slides were counterstained with hematoxylin.

Agarose gel cultures

Chondrocytes were cultured in agarose-stabilized suspension using a modified method as previously described [28]. Primary monolayer cultures were trypsinized, re-suspended in agarose gel medium : DMEM/F-12 containing 10% FBS, 100 units/ml penicillin G, 100 mg/ml streptomycin, and 50 mg/ml ascorbate, to a concentration of 2×10^4 cells/ml, then mixed with equal volume of 1% low-temperature melting agarose (Sigma-Aldrich, Steinheim, Germany) in agarose gel medium, giving a final concentration of 1×10^4 cells/ml suspended in 0.5% low-temperature melting agarose in agarose gel medium (suspension agarose). Three milliliters of suspension agarose were added to 60 mm culture plates that were precoated with 2 ml of 1% autoclaved standard agarose (Bio-Rad, Hercules, CA). The gel was allowed to solidify at 4°C before addition of agarose gel medium. Then, culture plates were placed in a 37°C, 5% CO_2 humidified incubator for 21 days, and medium containing indicated concentration of nicotine was replaced once at the beginning of the week. After 21 days, suspension agarose was transferred to a glass slide, and placed on a plate warmer at 50°C with a covering of positively-charged nylon membranes (Roche, Mannheim, Germany). The slides were completely dried in a incubator at 42°C overnight, and fixed in 4% paraformaldehyde for 15 min, and stained with ALB to identify colonies producing glycosaminoglycans and to observe histologically. Colonies were defined as a cluster of cells with a diameter greater than 50 µm. ALP activity was determined in non-fixed agarose slide by Histofine, ALP substrate kit (Nichirei, Tokyo, Japan) following the manufacturer's product information. Type 10 collagen expression was also determined in the agarose slide using specific monoclonal antibody (Sigma; product number: C7974). The slide was fixed in acetone (Nacalai Tesque, Kyoto, Japan) at room temperature for 20 min. Non-specific binding was blocked with 2.5% normal rabbit serum (DakoCytomation, Glostrup, Denmark) in PBS containing 1% BSA and 1% Triton X-100. Slides were incubated for 6 h at room temperature with primary antibody, diluted 1:2000 in PBS containing 1% BSA. Bound antibody was detected by HRP-conjugated polyclonal rabbit anti-mouse IgM antibody (Dako, Glostrup, Denmark; product number: P 0260) diluted 1:100 in PBS at room temperature for 30 min. Peroxidase activity was visualized with diaminobenzidine tetrahidrochloride plus 0.03% H_2O_2, and slide was counterstained with hematoxylin.

Alginate bead cultures

Chondrocytes were cultured in alginate beads following the method described by De Ceuninck et al. Primary monolayer cultures were trypsinized, washed, and centrifuged. The isolated chondrocytes were suspended at a concentration of 2×10^6 cells/ml in a 1.25% alginate in 0.15 M NaCl. The cell suspension was slowly expressed through a 21 gauge needle and dropped into a 102 mM $CaCl_2$ solution. The beads with approximately 25,000 cells/bead were allowed to polymerize for 10 min and washed three times with 0.15 M NaCl, followed by two washes in DMEM/F12. The beads were then transferred to medium (200 beads/10 ml/60 mm culture dish): DMEM/F-12 containing 10% FBS, 50 µg/ml ascorbate, 100 units/ml penicillin G, 100 mg/ml streptomycin. The beads were cultured at 37°C in a 5% CO_2 humidified incubator for four months, and medium with or without nicotine was replaced twice weekly. The beads were transferred to new dishes every other week to avoid the formation of monolayer cultures on the bottom of the dish by chondrocytes escaping from the beads.

For histological analysis, the beads were fixed in 4% paraformaldehyde, 0.1 M cacodylate buffer, pH 7.4, containing 10 mM $CaCl_2$ for 4 h at room temperature, and then washed overnight at 4°C in 0.1 M cacodylate buffer, pH 7.4, containing 50 mM $BaCl_2$. The beads were dehydrated through alcohols and embedded in paraffin. The sections were routinely stained with ALB and safranin-O.

For RT-PCR analysis, chondrocytes were separated from the beads by incubating the beads in dissolution solution (at a ratio of 200 µl/bead), containing 55 mM EDTA, for 5 min and centrifuged. Total RNA was isolated by using RNeasy (Qiagen) following manufacturer's instructions, and was converted to cDNA by same method as described above. The sequences of PCR primers of human chondrocyte-related gene are listed in Table S2. PCR was performed in a final volume of 50 µl containing 2 µl of the single strand cDNA product (10 ng/µl), 10 mM Tris-HCl (pH8.3), 50 mM KCl, 1.5 mM $MgCl_2$, 200 µM dNTPs, 1.25 U Taq (Takara), and 20 pmol of each forward (5′) and reverse (3′) primers.

Calcium imaging

Primary monolayer cultures in 35 mm glass-bottomed plates were prepared. At near confluence, measurement was done by using Fluo-4 NW calcium assay kit (Molecular Probes, product number: F36206) following the manufacturer's product information. In short, the cells were incubated in dye loading solution containing 2.5 mM probenecid at 37°C for 30 min, then at room temperature for an additional 30 min before nicotine stimulation. The fluorescence was measured in LSM 510 (Carl Zeiss) with the settings appropriate for argon laser. Nicotine and its antagonists were prepared as a solution in assay buffer. If antagonists were used, they were added 30 min prior to nicotine stimulation.

Maternal nicotine exposure in wild-type mice

Three-month-old pregnant mice were purchased at day 1 of pregnancy from Sankyo Laboratories (Tokyo, Japan). The mice were given drinking water containing 2% sucrose (Wako, Osaka, Japan) with or without nicotine (hydrogen tartrate salt; Sigma-

Aldrich, St. Louis, MO). Nicotine was added to the sucrose solution starting at an initial concentration of 25 μg/ml to the treatment group mice. This was increased to 50 μg/ml on days 3 to 4, 100 μg/ml after day 5. The control mice were given only sucrose solution as a drinking water. The pregnant mice were sacrificed at noon on gestational day 15. The embryo were immediately weighed, and the legs were immediately removed and fixed in 4% paraformaldehyde phosphate buffer solution (Wako) for 24 h. Then, the legs were dehydrated through alcohols, embedded in paraffin, and sections were stained with Hematoxylin and Eosin for histological analysis.

Maternal nicotine exposure in alpha7 nAChR-disrupted mice

B6.129S7-Chrna7<tm1Bay>/J, the alpha7 nAChR +/− mice were obtained from Charles River Laboratories Japan. Ten- to 12-week old alpha7 nAChR +/− mice were mated, and pregnant mice were given sucrose solution with or without nicotine. The fetuses were obtained and analyzed as in the case of wild-type C57BL/6J mice, as described above. The alpha7 nAChR genotype was determined by means of PCR reaction with the specific primers (Table S3).

Statistics

The results of the quantative assays were expressed as mean±S.D. Significance was determined with Student's *t* test and ANOVA. All experiments were replicated twice.

Supporting Information

Figure S1 In vivo chondrocytic proliferation assay. A: Paraffin section of the femur of E15.5 C57BL/6J mice immunohistochemically stained with antibody to PCNA. Proliferative chondrocytes extensively stained positive for PCNA regardless of maternal nicotine exposure. B: Percentage of PCNA-positive cells in chondrocytes of the proliferative zone. There is no significant difference between the two groups. Hind legs of E15.5 C57BL/6J mice were prepared, fixed in 4% paraformaldehyde phosphate buffer solution (Wako) overnight at 4°C, and embedded in paraffin. After deparaffinization, slides were autoclaved in 0.01 M citrate buffer (pH 6.0) for 10 min, incubated with primary antibody to PCNA (DAKO: PC10) diluted 1:400 in PBS containing 1% BSA at room temperature for 3 h, and incubated with polyclonal rabbit anti-mouse immunoglobrins/HRP (DAKO: P260) at room temperature for 1 h. Staining was undertaken using a solution containing diaminobenzidine and 0.01% H_2O_2 in 0.05 M Tris-HCl buffer at pH 6.7, followed by counterstaining with hematoxylin.

Found at: doi:10.1371/journal.pone.0003945.s001 (0.06 MB PDF)

Table S1 Primers for nAChR subunit genes

Found at: doi:10.1371/journal.pone.0003945.s002 (0.03 MB PDF)

Table S2 Primers for chondrocyte specific genes

Found at: doi:10.1371/journal.pone.0003945.s003 (0.01 MB PDF)

Table S3 Primers for genotypying alpha7 nAChR gene

Found at: doi:10.1371/journal.pone.0003945.s004 (0.01 MB PDF)

Acknowledgments

We would like to express our sincere thanks to M. Nasu, C-H. Cui, H. Akutsu, K. Miyado, and M. Toyoda for support throughout this work, to H. Abe for providing expert technical assistance, to K. Saito and Y. Ito for their secretarial work, and to A. Crump for reviewing the manuscript.

Author Contributions

Conceived and designed the experiments: AK AU. Performed the experiments: AK HM. Analyzed the data: AK HM AU. Contributed reagents/materials/analysis tools: KS HI ST YT. Wrote the paper: AK AU.

References

1. Davies DP, Abernethy M (1976) Cigarette smoking in pregnancy: Associations with maternal weight gain and fetal growth. Lancet 1: 385–387.
2. Hardy JB, Mellits ED (1972) Does maternal smoking during pregnancy have a long-term effect on the child? Lancet 2: 1332–1336.
3. Wingerd J, Schoen EJ (1974) Factors influencing length at birth and height at five years. Pediatrics 53: 737–741.
4. Karatza AA, Varvarigou A, Beratis NG (2003) Growth up to 2 years in relationship to maternal smoking during pregnancy. Clin Pediatr (Phila) 42: 533–541.
5. Sexton M, Hebel JR (1984) A clinical trial of change in maternal smoking and its effect on birth weight. Jama 251: 911–915.
6. Yerushalmy J (1971) The relationship of parents' cigarette smoking to outcome of pregnancy–implications as to the problem of inferring causation from observed associations. Am J Epidemiol 93: 443–456.
7. Olsen J, Pereira Ada C, Olsen SF (1991) Does maternal tobacco smoking modify the effect of alcohol on fetal growth? Am J Public Health 81: 69–73.
8. Trygg K, Lund-Larsen K, Sandstad B, Hoffman HJ, Jacobsen G, et al. (1995) Do pregnant smokers eat differently from pregnant non-smokers? Paediatr Perinat Epidemiol 9: 307–319.
9. Haddon W Jr, Nesbitt RE, Garcia R (1961) Smoking and pregnancy: carbon monoxide in blood during gestation and at term. Obstet Gynecol 18: 262–267.
10. Mochizuki M, Maruo T, Masuko K (1985) Mechanism of foetal growth retardation caused by smoking during pregnancy. Acta Physiol Hung 65: 295–304.
11. Nordstrom ML, Cnattingius S (1996) Effects on birthweights of maternal education, socio-economic status, and work-related characteristics. Scand J Soc Med 24: 55–61.
12. Mau G (1976) Letter: Smoking and the fetus. Lancet 1: 972.
13. Nelson E, Jodscheit K, Guo Y (1999) Maternal passive smoking during pregnancy and fetal developmental toxicity. Part 1: gross morphological effects. Hum Exp Toxicol 18: 252–256.
14. El-Zawawy HB, Gill CS, Wright RW, Sandell LJ (2006) Smoking delays chondrogenesis in a mouse model of closed tibial fracture healing. J Orthop Res 24: 2150–2158.
15. Olsen J (1992) Cigarette smoking in pregnancy and fetal growth. Does the type of tobacco play a role? Int J Epidemiol 21: 279–284.
16. Sharma G, Vijayaraghavan S (2002) Nicotinic receptor signaling in nonexcitable cells. J Neurobiol 53: 524–534.
17. Americ SP, Brioni JD (1999) Neuronal nicotinic receptors : pharmacology and therapeutic opportunities. New York: Wiley-Liss, xii, 421 p.
18. Tacchetti C, Quarto R, Nitsch L, Hartmann DJ, Cancedda R (1987) In vitro morphogenesis of chick embryo hypertrophic cartilage. J Cell Biol 105: 999–1006.
19. Hauselmann HJ, Fernandes RJ, Mok SS, Schmid TM, Block JA, et al. (1994) Phenotypic stability of bovine articular chondrocytes after long-term culture in alginate beads. J Cell Sci 107 (Pt1): 17–27.
20. Kurtoglu S, Gunes T, Koklu E, Bastug O, Canoz O, et al. (2007) Influence of maternal nicotine exposure on neonatal rat bone: protective effect of pentoxifylline. Exp Biol Med (Maywood) 232: 398–405.
21. Gullahorn L, Lippiello L, Karpman R (2005) Smoking and osteoarthritis: differential effect of nicotine on human chondrocyte glycosaminoglycan and collagen synthesis. Osteoarthritis Cartilage 13: 942–943.
22. Orr-Urtreger A, Goldner FM, Saeki M, Lorenzo I, Goldberg L, et al. (1997) Mice deficient in the alpha7 neuronal nicotinic acetylcholine receptor lack alpha-bungarotoxin binding sites and hippocampal fast nicotinic currents. J Neurosci 17: 9165–9171.
23. Arredondo J, Nguyen VT, Chernyavsky AI, Bercovich D, Orr-Urtreger A, et al. (2002) Central role of alpha7 nicotinic receptor in differentiation of the stratified squamous epithelium. J Cell Biol 159: 325–336.
24. Luck W, Nau H, Hansen R, Steldinger R (1985) Extent of nicotine and cotinine transfer to the human fetus, placenta and amniotic fluid of smoking mothers. Dev Pharmacol Ther 8: 384–395.

25. Dempsey D, Jacob P 3rd, Benowitz NL (2000) Nicotine metabolism and elimination kinetics in newborns. Clin Pharmacol Ther 67: 458–465.
26. Sano M, Umezawa A, Abe H, Akatsuka A, Nonaka S, et al. (2001) EAT/mcl-1 expression in the human embryonal carcinoma cells undergoing differentiation or apoptosis. Exp Cell Res 266: 114–125.
27. Sano M, Umezawa A, Suzuki A, Shimoda K, Fukuma M, et al. (2000) Involvement of EAT/mcl-1, an anti-apoptotic bcl-2-related gene, in murine embryogenesis and human development. Exp Cell Res 259: 127–139.
28. Benya PD, Shaffer JD (1982) Dedifferentiated chondrocytes reexpress the differentiated collagen phenotype when cultured in agarose gels. Cell 30: 215–224.

Gremlin Enhances the Determined Path to Cardiomyogenesis

Daisuke Kami[1,3], Ichiro Shiojima[4], Hatsune Makino[1], Kenji Matsumoto[2], Yoriko Takahashi[1], Ryuga Ishii[1], Atsuhiko T. Naito[4], Masashi Toyoda[1], Hirohisa Saito[2], Masatoshi Watanabe[3], Issei Komuro[4], Akihiro Umezawa[1]*

1 Department of Reproductive Biology, National Institute for Child Health and Development, Tokyo, Japan, 2 Department of Allergy and Immunology, National Institute for Child Health and Development, Tokyo, Japan, 3 Laboratory for Medical Engineering, Division of Materials Science and Chemical Engineering, Graduate School of Engineering, Yokohama National University, Yokohama, Japan, 4 Department of Cardiovascular Science and Medicine, Chiba University Graduate School of Medicine, Chiba, Japan

Abstract

Background: The critical event in heart formation is commitment of mesodermal cells to a cardiomyogenic fate, and cardiac fate determination is regulated by a series of cytokines. Bone morphogenetic proteins (BMPs) and fibroblast growth factors have been shown to be involved in this process, however additional factors needs to be identified for the fate determination, especially at the early stage of cardiomyogenic development.

Methodology/Principal Findings: Global gene expression analysis using a series of human cells with a cardiomyogenic potential suggested *Gremlin* (*Grem1*) is a candidate gene responsible for *in vitro* cardiomyogenic differentiation. Grem1, a known BMP antagonist, enhanced DMSO-induced cardiomyogenesis of P19CL6 embryonal carcinoma cells (CL6 cells) 10–35 fold in an area of beating differentiated cardiomyocytes. The Grem1 action was most effective at the early differentiation stage when CL6 cells were destined to cardiomyogenesis, and was mediated through inhibition of BMP2. Furthermore, BMP2 inhibited Wnt/β-catenin signaling that promoted CL6 cardiomyogenesis.

Conclusions/Significance: Grem1 enhances the determined path to cardiomyogenesis in a stage-specific manner, and inhibition of the BMP signaling pathway is involved in initial determination of Grem1-promoted cardiomyogenesis. Our results shed new light on renewal of the cardiovascular system using Grem1 in human.

Citation: Kami D, Shiojima I, Makino H, Matsumoto K, Takahashi Y, et al. (2008) Gremlin Enhances the Determined Path to Cardiomyogenesis. PLoS ONE 3(6): e2407. doi:10.1371/journal.pone.0002407

Editor: Hernan Lopez-Schier, Centre de Regulacio Genomica, Spain

Received January 15, 2008; **Accepted** May 5, 2008; **Published** June 11, 2008

Copyright: © 2008 Kami et al. This is an open-access article distributed under the terms of the Creative Commons Attribution License, which permits unrestricted use, distribution, and reproduction in any medium, provided the original author and source are credited.

Funding: This study was supported by a grant from the Ministry of Education, Culture, Sports, Science and Technology (MEXT) of Japan and Health and Labor Sciences Research Grants; by a Research grant on Health Science Focusing on Drug Innovation from the Japan Health Science Foundation; by the Program for Promotion of Fundamental Studies in Health Science of the Pharmaceuticals and Medical Devices Agency; by a grant from the Terumo Life Science Foundation; by a Research Grant for Cardiovascular Disease from the Ministry of Health, Labor and Welfare (MHLW); and by a Grant for Child Health and Development from the MHLW.

Competing Interests: The authors have declared that no competing interests exist.

* E-mail: umezawa@1985.jukuin.keio.ac.jp

Introduction

The critical event in heart formation is commitment of mesodermal cells to a cardiomyogenic fate and their migration into anterolateral regions of the embryo during late gastrulation. In this process, morphogenic movements and cardiac fate determination are regulated by cytokines such as bone morphogenetic proteins (BMPs) [1–3], and fibroblast growth factors (FGFs) [4–7]. These secreted proteins from neighboring endoderm, ectoderm, and the mesoderm itself, play important roles in induction of cardiac transcription factors [8] and differentiation of cardiomyocytes in amphibians [9] and avians [4]. Cardiomyogenic signals, such as BMPs and FGFs, indeed activate expression of cardiac specific transcriptional factors (Csx/Nkx2.5, Gata4, Mef2c), and these transcriptional factors activate expression of circulating hormones (atrial natriuretic peptide (ANP), brain natriuretic peptide (BNP)), and cardiac specific proteins (myosin heavy chain (MyHC), myosin light chain (MyLC)). Wnt family proteins, cysteine-rich, and secreted glycoproteins, have also been implicated in embryonic development [10,11], and cardiomyogenesis [12,13]. In *Drosophila*, '*wingless*', a homologue of vertebrate Wnt is involved in expression of '*tinman*', a *Drosophila* homologue of Csx/Nkx2.5, through '*armadillo*', a *Drosophila* ortholog of β-catenin, and drives heart development [14]. In vertebrates, however, Wnt1/3a, which activates the canonical Wnt/β-catenin signaling pathway leading to stabilization of β-catenin as a downstream molecule through inactivation of glycogen synthase kinase-3β, inhibits cardiomyocytic differentiation from cardiac mesoderm [15–18]. Wnt11 promotes cardiac differentiation via the non-canonical pathway in *Xenopus* [12] and murine embryonic cell lines [19]. The secretion of Wnt inhibitors such as 'Cerberus', 'Dickkopf' and 'Crescent' by the anterior endoderm prevents Wnt3a secreted by the neural tube from inhibiting heart formation [15–17].

In this study, we performed GeneChip analysis to identify multiple extracellular determinants, such as cytokines, cell

membrane-bound molecules and matrix responsible for cardiomyogenic differentiation, and evaluated the statistical significance of differential gene expression by NIA array analysis (http://lgsun.grc.nia.nih.gov/ANOVA/) [20], a web-based tool for microarray data analysis. We found that Grem1 enhances the determined path to cardiomyogenesis in a stage-specific manner, and that inhibition of the BMP signaling pathway is, at least in part, involved in initial determination of Grem1-promoted cardiomyogenesis.

Results

GeneChip and statistical analysis

To identify cytokines and transcription factors responsible for cardiomyogenic differentiation, 69 human cells were analyzed, depending on gene expression levels, by GeneSpringGX software, and clustered into 30 groups (Fig. 1A, Table 1). Among the 30 groups, 21 groups included cells with a cardiomyogenic potential (Fig. 1B: red numbers). To identify genes specific for these groups, hierarchical clustering was employed, using the average distance method. Genes with the lowest average expression E(G1) within the cluster that can differentiate into cardiomyocytes and genes with the highest average expression E(G2) outside the cluster were identified, as previously described [20–22]. Genes which have E(G1)>E(G2) were estimated, using the False Discovery Rate (FDR<0.05). Grem1 was nominated as a cluster-specific cardiomyocyte-promoting gene in cells that could differentiate into cardiomyocytes following NIA array analysis (Fig. 1B). The gene expression profile reported in this paper has been deposited in the Gene Expression Omnibus (GEO) database (http://www.ncbi.nlm.nih.gov/geo: accession no. GSE8481, GSM41342-GSM41344, and GSM201137- GSM201145).

Cardiomyogenic differentiation of CL6 cells with Grem1 and DMSO

To investigate cardiomyogenic activity of Grem1, P19CL6 embryonal carcinoma cells (CL6 cells) were used for assessment of *in vitro* cardiomyogenic differentiation, since CL6 cells are reproducibly and stably induced into beating cardiomyocytes by DMSO (Fig. 2Aa) [23]. CL6 cells did not differentiate following exposure to Grem1 alone at concentrations of 63 or 125 ng/ml for 14 days (Fig. 2B). However, Grem1 dramatically promotes DMSO-induced cardiomyogenic differentiation at a concentration of 63 and 125 ng/ml; Grem1 (125 ng/ml) especially increased DMSO-induced cardiomyogenic differentiation of CL6 cells as assessed by beating area (Fig. 2Ab and B) (Movie S1 and S2, http://1954.jukuin.keio.ac.jp/umezawa/kami/index.html).

RT-PCR of differentiated or undifferentiated CL6 cells

To investigate gene expression as well as morphological analysis, i.e. beating, during cardiomyogenic differentiation, RT-PCR analysis was performed to detect expression of cardiomyocyte-specific/associate transcription factors, and structural genes (Fig. 2C). Genes encoding *Csx/Nkx2.5*, *Gata4*, *Hand2*, *Mef2c*, *ANP*, *BNP*, *MyLC-2a*, *MyLC-2v*, and *β-MyHC* were up-regulated during cardiomyogenic differentiation of CL6 cells treated with Grem1 and DMSO (Fig. 2C: lanes 6, 7 versus lane 3). Triplicate independent experiments confirmed the concentration-dependent Grem1 action on cardiomyogenic differentiation. The cardiomyocyte-specific genes (*Csx/Nkx2.5*, *Gata4*, *MyLC-2a*, *MyLC-2v*) expression level of CL6 cells treated with DMSO and Grem1 (63 and 125 ng/ml) were also the same as or higher than that of DMSO-induced CL6 cells by semi-quantitative RT-PCR (Figure S1).

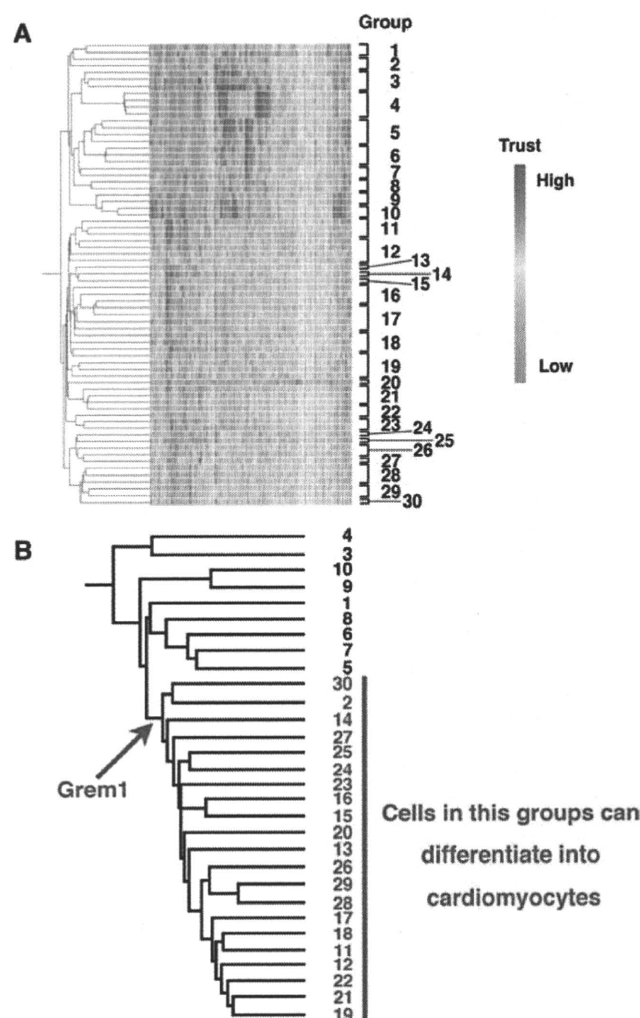

Figure 1. Hierarchical clustering analysis on cultured human cells. (A) Hierarchical clustering analyzed by GeneSpring. Based on gene expression pattern, 69 human cells were clustered into 30 sub-groups. The raw data from the GeneChip analysis are available at the GEO database with accession number GSE8481, GSM41342- GSM41344, and GSM201137- GSM201145. **(B)** Hierarchical clustering analysis was performed by NIA array (http://lgsun.grc.nia.nih.gov/ANOVA/), using averaged values of 30 sub-groups. Among the 30 groups, 21 groups included cells with a cardiomyogenic potential. To identify genes specific for these groups, hierarchical clustering was employed. *Grem1* was nominated as a cluster-specific cardiomyocyte-promoting gene in cells that could differentiate into cardiomyocytes.
doi:10.1371/journal.pone.0002407.g001

Immunocytochemistry of differentiated or undifferentiated CL6 cells

To examine CL6 cells for expression of cardiomyocytic protein, immunocytochemical analysis was performed. CL6 treated with Grem1 (125 ng/ml) and DMSO exhibited clear striation with immunostain using anti-cTnT or anti-α-actinin (Fig. 2Da and b). The MF20- and cTnT-positive cells after exposure to Grem1 and DMSO formed clusters (Fig. 2Ea), compared with the cells after exposure to DMSO alone (Fig. 2Eb). CL6 cells treated with Grem1 alone were negative for MF20 and cTnT, but became positive for both markers following exposure to Grem1 (63 and 125 ng/ml) and DMSO (Fig. 2F). The beating area (Fig. 2B) showed a tendency similar to the MF20- and cTnT-positive area (Fig. 2F), thus there were positive correlations between them.

Table 1. 69 human cells clustered into 30 groups

Group		Title	Description	GSM
1	Normal epithelial cell,primary	NHEK-Neo1	Normal epidermal keratinocyte, neonate, primary	GSM210361
		NHBE-1	Normal bronchial epithelial cell, primary	GSM210362
2	Pulmonary epithelial cell line	A549	Pulmonary epithelial cell line	GSM210363
		BEAS-2B control (6hr)	Bronchial epithelial cell line	GSM210364
3	Lymphocyte	RPMI8226control (6hr)	B cell line	GSM210365
		Raji-1	B cell line	GSM210366
		NK92	NK cell line	GSM210367
4	Myelomonocytic leukemia	U937c	U937 control	GSM210368
		U937h	U937+HRF	GSM210369
		U937ha	U937+HRF+antibody	GSM210370
		U937a	U937+antibody	GSM210371
5	Embryonal carcinoma, cancer	NCR-G3	Embryonal carcinoma, NCR-G3, non-adherent	GSM201141
		NCR-G2NAd	Embryonal carcinoma, NCR-G2, non-adherent	GSM210373
		NCR-G4Ad	Embryonal carcinoma, NCR-G4, adherent	GSM201142
		NCR-G3Ad	Embryonal carcinoma, NCR-G3, adherent	GSM210375
6	ES cell	H1_P43	Undifferentiated hES	GSM41342
		H1-P46	Undifferentiated hES	GSM41343
		H1-P41	Undifferentiated hES	GSM41344
7	Embryonal carcinoma, cancer	NCR-G2Ad	Embryonal carcinoma, NCR-G2, adherent	GSM201140
		NCR-G1	Embryonal carcinoma, NCR-G3, non-adherent	GSM201139
8	Ewing, cancer	NCR-EW2	Ewing, cancer	GSM210378
		NCR-EW3	Ewing, ETV4, cancer	GSM210379
9	Ewing, cancer	GST6	Ewing, POU5F1, cancer	GSM201137
		GST6-extra	Ewing, POU5F1, cancer	GSM210381
10	Ewing, cancer	GST6-5az	Ewing, POU5F1, 5azaC, cancer	GSM201138
		GST6-5az-extra	Ewing, POU5F1, 5azaC, cancer	GSM210383
11	Bone marrow cell, primary	H4-1	Bone marrow cell, primary	GSM201143
		UBT5	Bmi-1, hTERT, bone marrow cell	GSM210385
		UBET7	Bmi-1, E6, hTERT, bone marrow cell	GSM210386
12	Ligament-derived cells	#10	Ligament, primary	GSM210387
	Marrow stromal cells	H10-2Vec	Vector, bone marrow cell	GSM210388
		H10-2TERT	hTERT, bone marrow cell	GSM210389
		H10-2Bmi1	Bmi-1, bone marrow cell	GSM210390
13	Placenta, primary	PL90	Placenta, primary	GSM210391
14	De-differentiated chondrocyte	TdHC1	E6, E7, hTERT, de-differentiated chondrocyte	GSM210392
15	Neural differentiated marrow stromal cell	UET13 Neural differentiation	E7, hTERT, neural differentiation, bone marrow cell	GSM210393
16	Neural differentiated marrow stromal cell	UET13 Neural differentiation1	E7, hTERT, neural differentiation, bone marrow cell	GSM210394
		UET13 Neural differentiation4	E7, hTERT, neural differentiation, bone marrow cell	GSM210395
		UET13 Neural differentiation5	E7, hTERT, neural differentiation, bone marrow cell	GSM210396
17	Cord blood-derived cells	UET13	E7, hTERT, bone marrow cell	GSM210397
		UCB408	Cord blood, primary	GSM210398
		UCB408E6E7-31	E6, E7, umbilical cord blood	GSM210399
	Adipocyte cell, primary	HAdPC1(5/21)	HAdpc1E6E7TERT28	GSM210400
18	Marrow mesenchymal cell, primary	UEET12	E6, E7, hTERT, bone marrow cell	GSM210401
		UEE16	E6, E7, bone marrow cell	GSM210402
		EPC hTERT+1	E6, E7, hTERT, endometrial cell	GSM201144
19	Cord blood, primary	UCB302	Cord blood, primary	GSM210382
		UCB302-D7	Cord blood, primary	GSM210405
		UCB302TERT	hTERT, cord blood	GSM210406
		UET9	E7, hTERT, bone marrow cell	GSM210407

Table 1. cont.

Group		Title	Description	GSM
20	Cord blood, primary	UCB408E7-32	E7, hTERT, cord blood	GSM210408
21	Fetal fibroblast, primary	HFDPC cont.	Normal follicular dermal papillar cell, primary	GSM210409
		PL112	Placenta, primary	GSM210410
		HF7-3	Fetal fibroblast, primary	GSM210411
22	Bone marrow cell, primary	3F0664	Bone marrow cell (commercial item), primary	GSM201145
		BM-MSC	Bone marrow-derived mesenchymal stem cells	GSM38627
23	ES cell-derived mesenchymal cell	H1 clone 2	ES cell-derived mesenchymal precursor	GSM38628
		H9 clone 1	ES cell-derived mesenchymal precursor	GSM38629
24	Endometrial cell	EPC100	E6, E7, hTERT, endometrial cell	GSM210413
25	Bone marrow cell, primary	Yub10F	Bone marrow cell, primary	GSM210414
26	Endometrial cell	EPC hTERT+2	E6, E7, hTERT, endometrial cell	GSM210415
		EPC Control	E6, E7, hTERT, endometrial cell	GSM210416
27	Endometrial cell	EPC214	E6, E7, hTERT, endometrial cell	GSM210417
28	Menstruation blood-derived mesenchymal cell, primary	#E4	Menstruation blood, primary	GSM210418
		#E4HRF	Menstruation blood, HRF treatment, primary	GSM210419
		#E5HRF	Menstruation blood, HRF treatment, primary	GSM210420
29	Menstruation blood-derived mesenchymal cell, primary	#E6	Menstruation blood, primary	GSM210421
		#E6HRF	Menstruation blood, HRF treatment, primary	GSM210422
30	Menstruation blood-derived mesenchymal cell, primary	#E5	Menstruation blood, primary	GSM210423

doi:10.1371/journal.pone.0002407.t001

Grem1 and DMSO were most effective at the early stage (days 1–3) of CL6 differentiation

To determine if Greml (125 ng/ml) functions during the early or the late stage of differentiation, CL6 cells were treated with Greml for different time periods (Fig. 3A). Greml and DMSO were most effective on CL6 differentiation at 1–3 days (Fig. 3B, C) as assessed by percentages of MF20-positive area and beating area. Since Greml inhibits BMPs through direct binding [24], we hypothesized that BMP signaling is inhibitory to CL6 cardiomyogenesis during days 1–3. To confirm this hypothesis, RT-PCR analysis was performed to determine expression of the early mesodermal marker (*BrachyuryT* and *Tbx6*), cardiomyocyte-specific transcription factors (*Csx/Nkx2.5*), structural genes (*β-MyHC*), and *Gapdh* (Fig. 4A). DMSO induced the *BrachyuryT* and *Tbx6* genes, and their expressions peaked at 3 days and then decreased; BMP2 down-regulated expression of these genes at 3–7 days. The *Csx/Nkx2.5* and *β-MyHC* genes started to be expressed at days 3 and 5, respectively, and their expression increased up to 14 days, at which time the timeframe analysis was terminated. BMP2 clearly inhibited expression of the *Csx/Nkx2.5* and *β-MyHC* genes (Fig. 4A, lanes 1–7 versus lanes 8–14).

To examine cardiomyogenic differentiation, immunocytochemical analysis was performed on CL6 cells treated with the inducers. CL6 cells treated with DMSO and BMP2 for the first 3 days were negative for sarcomeric myosin (MF20) at 14 days, but became positive for sarcomeric myosin, following exposure to DMSO alone during days 1–3 (Fig. 4B). To determine if DMSO induces BMP production in CL6 cells, expression levels of *Bmp2* and *Bmp4* were determined by quantitative real-time RT-PCR analysis (Fig. 4C). DMSO clearly induced the *Bmp2* and *Bmp4* genes, and DMSO-induction was inhibited by BMP2 protein. The expression level of *Bmp2* was highest during days 7–10 (Fig. 4C: *Bmp2*) in DMSO-induced CL6 cells, and that of *Bmp4* was highest during days 5–7 (Fig. 4C: *Bmp4*).

To investigate BMP signaling on cardiomyogenic differentiation, we used the *Id1* promoter-Lux plasmid that includes the luciferase gene driven by the *Id1* promoter, known as a BMP target promoter (Fig. 4D). DMSO increased BMP signaling activity that peaked at 5 days (Fig. 4D, open square). BMP2 protein increased BMP signaling activity at 3 days (Fig. 4D, closed square), but lost BMP signaling activity at 5 days and later, implying that this loss of BMP signaling leads to lack of cardiomyogenic induction.

Since Wnt/β-catenin signaling is involved in CL6 cardiomyogenesis [23,25], we hypothesized that the BMP effect on CL6 cardiomyogenesis is mediated through Wnt/β-catenin signaling. Expression of Wnt3a, an activator of canonical Wnt signaling, was indeed detected in CL6 cells exposed to DMSO, and BMP2 significantly down-regulated *Wnt3a* expression at day 3 (Fig. 4E). By using the TOPflash plasmid [23] which includes the luciferase gene driven by two sets of three copies of the TCF recognition site, Wnt/β-catenin signaling was assessed to investigate the effect of BMP2. Wnt/β-catenin signaling activity increased at 48 h after treatment with DMSO. Activity was increased by DMSO treatment but decreased by BMP2 (Fig. 4F). Time course analysis revealed that Wnt/β-catenin activity peaked at 5 days after DMSO treatment, and decreased thereafter (Fig. 4G). BMP2 inhibited DMSO-induced Wnt/β-catenin activity throughout the experimental period (up to 14 days). These results imply that BMP signaling inhibits CL6 cardiomyogenesis at the early stage through inhibition of Wnt/β-catenin signaling.

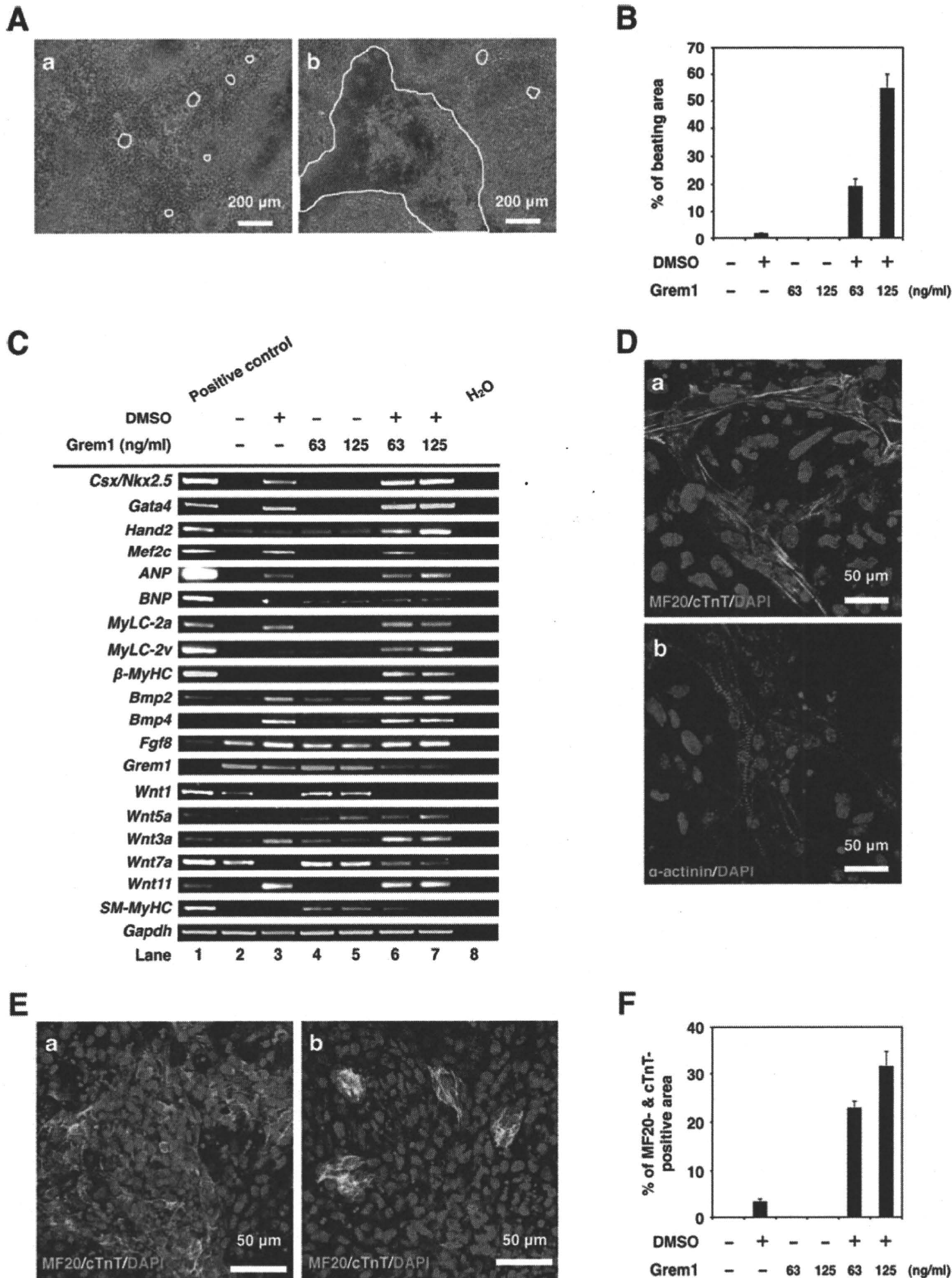

Figure 2. Grem1 enhanced cardiomyogenic differentiation in DMSO-induced CL6 cells. (A) Phase contrast micrograph of CL6 cells with exposure to DMSO alone (a), Grem1 (125 ng/ml) and DMSO (b) for 14 days. The medium, including Grem1 and DMSO, was changed every day. CL6 cells exhibited apparent spontaneous beating between days 9–11. Beating CL6 cell colonies are outlined by white lines. **(B)** Percentage of beating area in differentiated CL6 cells. CL6 cell treated with Grem1 (125 ng/ml) and DMSO exhibited the strongest contraction. **(C)** RT-PCR analysis of the genes encoding cardiac-specific transcriptional factors (*Csx/Nkx2.5, Gata4, Mef2c, Hand2*), circulating hormone (*ANP, BNP*), cardiac-specific proteins (*MyLC-2a, MyLC-2v, β-MyHC*), cytokines (*Bmp2, Bmp4, Fgf8, Grem1, Wnt1, Wnt3a, Wnt5a, Wnt7a, Wnt11*), *SM-MyHC*, and *Gapdh* (From top to bottom). Mouse total heart RNA for the *Csx/Nkx2.5, Gata4, Mef2c, Hand2, ANP, BNP, MyLC-2a, MyLC-2v, β-MyHC, Bmp2, Bmp4, Grem1, Wnt11, SM-MyHC*, and *Gapdh* genes, mouse embryonic stem cell RNA for the *Fgf8* gene, and mouse total skeletal muscle RNA for the *Wnt1, Wnt3a, Wnt5a*, and *Wnt7a* genes were used for positive controls. H_2O (without RNA) served as a negative control. **(D)** Immunocytochemistry of CL6 cells 14 days after exposure to Grem1 (125 ng/ml) and DMSO with MF20 and cTnT (a), and α-actinin (b). Cell nuclei are stained with DAPI. Clear striations are evident. **(E)** Immunocytochemistry of CL6 cells 14 days after exposure to Grem1 and DMSO with cardiac troponin T (cTnT) and sarcomeric myosin (MF20). CL6 cells treated with Grem1 (125 ng/ml) and DMSO (a), and DMSO alone (b) stained positive for cTnT and MF20. Untreated CL6 cells, i.e. not exposed to Grem1(125 ng/ml) or DMSO, stained negative for cTnT and MF20. Cell nuclei were stained with DAPI. **(F)** Percentage of MF20- and cTnT-double positive area.
doi:10.1371/journal.pone.0002407.g002

A

	Day	0	1	2	3	4	5	6	7	8	9	10	11	12	13	14
DMSO	–	–	–	–	–	–	–	–	–	–	–	–	–	–	–	–
Grem1	–	–	–	–	–	–	–	–	–	–	–	–	–	–	–	–
DMSO	1-14	–	+	+	+	+	+	+	+	+	+	+	+	+	+	+
Grem1	–	–	–	–	–	–	–	–	–	–	–	–	–	–	–	–
DMSO	1-14	–	+	+	+	+	+	+	+	+	+	+	+	+	+	+
Grem1	1-3	–	+	+	+	–	–	–	–	–	–	–	–	–	–	–
DMSO	1-14	–	+	+	+	+	+	+	+	+	+	+	+	+	+	+
Grem1	4-7	–	–	–	–	+	+	+	+	–	–	–	–	–	–	–
DMSO	1-14	–	+	+	+	+	+	+	+	+	+	+	+	+	+	+
Grem1	8-14	–	–	–	–	–	–	–	–	+	+	+	+	+	+	+
DMSO	1-3		+	+	+	–	–	–	–	–	–	–	–	–	–	–
Grem1	–	–	–	–	–	–	–	–	–	–	–	–	–	–	–	–
DMSO	1-14	–	+	+	+	+	+	+	+	+	+	+	+	+	+	+
Grem1	1-14	–	+	+	+	+	+	+	+	+	+	+	+	+	+	+
DMSO	1-14	–	+	+	+	+	+	+	+	+	+	+	+	+	+	+
Grem1	1-3	–	+	+	+	–	–	–	–	–	–	–	–	–	–	–
DMSO	1-3	–	+	+	+	–	–	–	–	–	–	–	–	–	–	–
Grem1	1-3	–	+	+	+	–	–	–	–	–	–	–	–	–	–	–

B

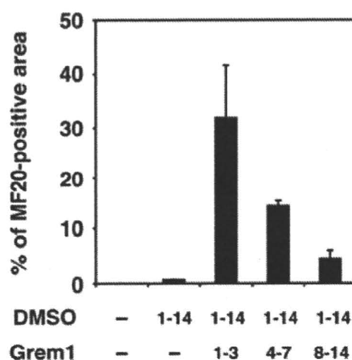

C

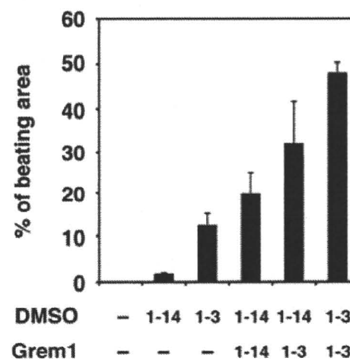

Figure 3. Percentage of myogenic differentiation by period of treatment with Grem1 in CL6 cells. (A) Protocol for treatment of Grem1 and DMSO. CL6 cells were passaged at 1.8×10^5 cells in 6-well plate on Day 0. CL6 cells were exposed to Grem1 (125 ng/ml) and/or DMSO on the indicated day. Day when the cells were exposed to the inducers is shown by "+" (in gray cells for clarity). The medium including Grem1 and DMSO was changed every day. On day 14, the cells were immunocytochemically stained with MF20 antibody. **(B)** Myogenic differentiation of CL6 cells was estimated by sarcomeric myosin (MF20)-positive area. CL6 cells were treated with Grem1 (125 ng/ml) and DMSO for the indicated days. **(C)** Myogenic differentiation of CL6 cells was estimated by beating area. CL6 cells treated with DMSO and Grem1 (125 ng/ml) were incubated at indicated days.
doi:10.1371/journal.pone.0002407.g003

Discussion

Our bioinformatics study using the results from the global gene expression analysis of human cells (GSM412342-41344 and GSM201137-201145 at http://www.ncbi.nlm.nih.gov/geo) nominated Greml as a candidate gene that may participate in cardiomyogenesis. By using CL6 embryonic cells as a model of cardiomyogenesis, we obtained two major findings: the first is that Greml enhanced cardiomyogenic differentiation of DMSO-induced CL6 cells at the early stage; the second is that Wnt/β-catenin and BMP signaling activity had developmental stage-specific effects on cardiomyogenesis (Fig. 5). Wnt/β-catenin activity at the early stage enhanced embryonic cell differentiation into cardiomyocytes, while suppressing this activity by BMP2 or BMP4 proteins as reported in the avian embryo [26]. In contrast, BMP signaling activity in the late stage enhanced cardiomyocytic differentiation. Greml regulated the stage-specific Wnt/β-catenin and BMP signaling activity on cardiomyogenesis.

Many studies have indicated that Greml is involved in cell differentiation and development, such as osteogenesis [27], lung morphogenesis [28], myogenesis [29], and limb formation [30], through inhibition of BMP2 and BMP4. Greml-null mice show intact heart development, despite impairment of lung and kidney [31], and therefore Greml is considered not to be involved in cardiogenesis, or supplementary factors such as Noggin [32], with a similar function, may compensate Greml during development. Greml had an enhancing or promoting activity in *in vitro* cardiomyogenesis, as is the case with platelet-derived growth factor as a promoter of cell growth [33]. In this study, Greml was involved in cardiomyocyte differentiation. However Greml alone could not induce cardiomyocytic differentiation of CL6 cells in the absence of DMSO (Fig. 2C and F), suggesting that Greml is solely

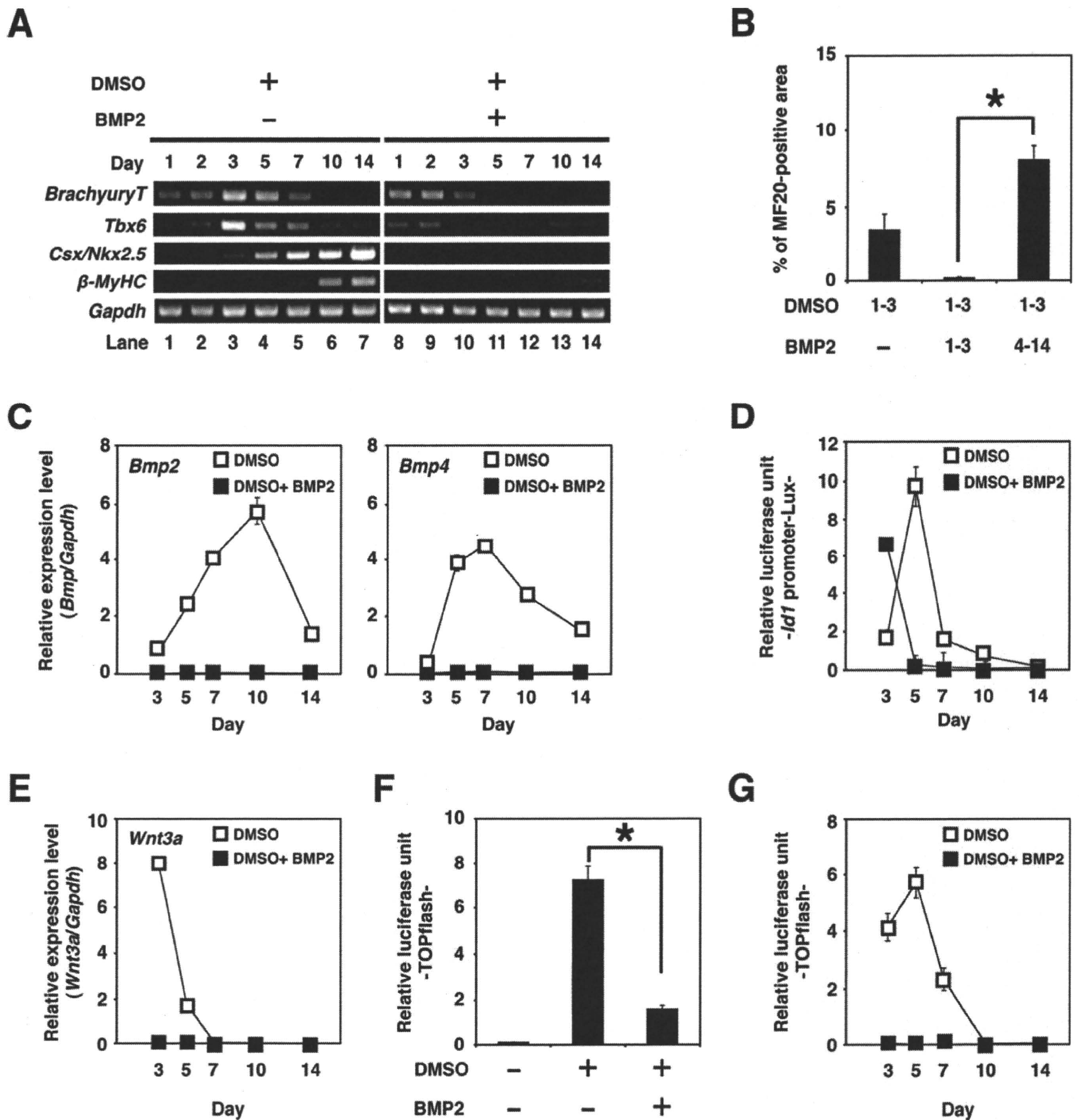

Figure 4. Cardiomyogenic differentiation in CL6 cells (days 1–3) is inhibited by BMP2. (A) RT-PCR analysis of the gene encoding *BrachyuryT*, *Tbx6*, cardiac-specific transcriptional factor (*Csx/Nkx2.5*), cardiac-specific protein (*β-MyHC*), and *Gapdh* (From top to bottom) of CL6 cells treated with DMSO alone, or DMSO and BMP2 (100 ng/ml) for the first 3 days (days 1–3). The medium, including BMP2 and DMSO, was changed every day. **(B)** Percentage of MF20-positive area. Immunocytochemistry was carried out on CL6 cells 14 days after cells had been exposed to DMSO and BMP2 (100 ng/ml) for the first 3 days (days 1–3). The asterisk indicates a significant statistical difference ($P<0.05$). **(C)** Quantitative real-time RT-PCR analysis of the gene encoding *Bmp2* (left), and *Bmp4* (right) in CL6 cells treated with DMSO alone (open square), or DMSO and BMP2 (100 ng/ml) (closed square) for the first 3 days (days 1–3). **(D)** BMP signaling activity of CL6 cells treated with DMSO alone (open square), or DMSO and BMP2 (100 ng/ml) (closed square) for the first 3 days (days 1–3) were determined by luciferase activity analysis using *Id1* promoter-Lux (a firefly luciferase reporter plasmid driven by the Id1 binding sites), pRL-CMV as co-transfected control, and Dual luciferase reporter assay system. Relative luciferase unit of the CL6 cells untreated with inducers at day 3 is regarded as 0.1 (data not shown). **(E)** Quantitative real-time RT-PCR analysis of the gene encoding *Wnt3a* in CL6 cells treated with DMSO alone (open square), or DMSO and BMP2 (100 ng/ml) (closed square) for the first 3 days (days 1–3). **(F)** Wnt/β-catenin signaling activity of CL6 cells 48 h after exposure to DMSO, or DMSO and BMP2 (100 ng/ml) was determined by luciferase activity analysis using TOPflash (a firefly luciferase reporter plasmid driven by two sets of three copies of the TCF binding site and herpes simple virus thymidine kinase minimal promoter), pRL-CMV as co-transfected control, and Dual luciferase reporter assay system. Relative luciferase unit of the CL6 cells untreated with inducers is regarded as 0.1. The asterisk indicates a significant statistical difference ($P<0.05$). **(G)** Timeframe of Wnt/β-catenin signaling activity in CL6 cells treated with DMSO alone (open square), or DMSO and BMP2 (100 ng/ml) (closed square) for the first 3 days (days 1–3). Relative luciferase unit of the CL6 cells untreated with inducers at day 3 is regarded as 0.1 (data not shown).
doi:10.1371/journal.pone.0002407.g004

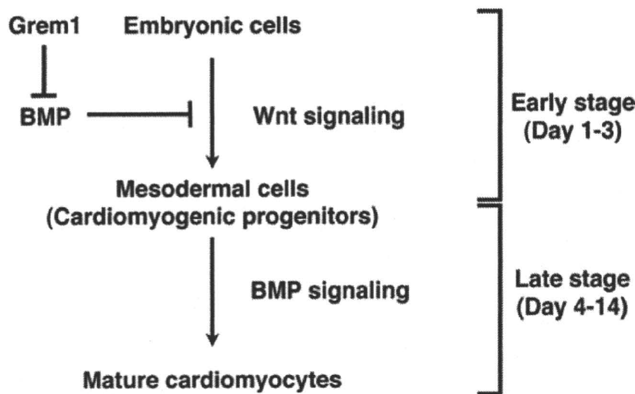

Figure 5. Grem1-accelerated CL6 cardiomyogenesis through regulation of BMP- and Wnt/β-catenin-signaling pathways. CL6 embryonic cells start to differentiate into mesodermal cells through Wnt/β-catenin signaling pathway at the early stage (days 1–3), and mesodermal CL6 cells differentiate into mature cardiomyocytes by BMP pathway at the late stage (days 4–14). Grem1 accelerates DMSO-induced cardiomyogenesis through inhibition of the BMP-signaling pathway.
doi:10.1371/journal.pone.0002407.g005

a promoter of cardiomyogenic differentiation. One of the possible mechanisms for Greml-enhanced cardiomyogenesis at the early stage is inhibition of the BMP signaling pathway [3]. Alternatively, Greml-enhanced cardiomyogenesis may be mediated through proliferation of cardiac progenitor cells, as is the case of myogenic progenitor proliferation by Greml [34], and this possibility is supported by an increased number of sarcomeric myosin-positive CL6 cardiomyocytes (Fig. 2E and F).

The stage specificity of the Greml effect is possibly correlated with the biphasic and antagonistic effect of Wnt/β-catenin signaling on cardiomyogenesis, depending on the stage of development *in vitro* [25] and *in vivo* [35]. CL6 cells differentiated into cardiomyocytes via mesodermal induction by the Wnt/β-catenin signaling pathway at the early stage, and CL6 mesodermal cells differentiated into cardiomyocytes induced by BMP2 at the late stage. It is conceivable that embryonic cells, such as CL6 cells and ES cells, differentiate into cardiomyocytes by inhibiting BMP signaling via putative "mesodermal cells" or "cardiomyogenic progenitors", or differentiation stages corresponding to these cells (Fig. 5, Figure S2). The early stage process from embryonic cells to mesodermal cells was mediated via Wnt/β-catenin signaling (Fig. 4F, G), and was assessed by expression of *BrachyuryT* and *Tbx6* genes (Fig. 4A), which are target genes for Wnt/β-catenin signaling [36]. BMP signaling antagonizes the cell fate-inducing activity of Wnt/β-catenin [37]. When embryonic cells or cardiomyogenic progenitors are induced to become mature cardiomyocytes by cytokines and growth factors, we must be careful with respect to the stage of cell differentiation because of the biphasic differential action of the factors which are dependent upon the differentiation stage.

In conclusion, we have demonstrated that Greml enhances the commitment or determined path to cardiogenic differentiation of CL6 teratocarcinoma cells. Apart from a role in development, Greml may serve a clinical use in cardiology, like granulocyte colony-stimulating factor that accelerates production of granulocytes in both peripheral blood and bone marrow. Nomination of *Greml* as a cardiomyogenic factor is based on hierarchical clustering analysis using global gene expression data of human cells. This bioinformatics approach may be useful for identifying morphogens/factors that can induce differentiation of other cell types/tissues/organs.

Materials and Methods

GeneChip analysis

GeneChip analysis was performed (Fig. 1A, Table 1) as previously described [38]. Human genome-wide gene expression was examined with the Human Genome U133A Probe array (GeneChip; Affymetrix), which contains the oligonucleotide probe set for approximately 23,000 full-length genes and expressed sequence tags, according to the manufacturer's protocol (Expression Analysis technical manual and GeneChip Small Sample Target Labeling Assay version 2 technical note [http://www.affymetrix.com/support/technical/index.affx]). Data analysis was performed by the GeneChip Operation System (Affymetrix) and GeneSpringGX software (Silicon Genetics). To normalize the staining intensity variations between chips, the average difference values for all genes on a given chip were divided by the median of all measurements on that chip. Hierarchical-clustering analysis was performed using a minimum distance value of 0.001, a separation ratio of 0.5, and the standard definition of the correlation distance.

Cell culture and differentiation

CL6 cells were grown on 100 mm dishes (Becton Dickinson) in α-MEM (Gibco) supplemented with 10% fetal bovine serum (FBS) (JRH Bioscience, Inc.), penicillin, and streptomycin, and were maintained in a 5% CO_2 atmosphere at 37°C. To induce differentiation, CL6 cells were plated at a density of 1.8×10^5 cells in a 6-well plate (Becton Dickinson) or gelatin-coated 35 mm glass base dishes (IWAKI) with α-MEM containing Greml (63 or 125 ng/ml: R&D system) and/or 1% dimethyl sulfoxide (DMSO) for 14 days. Recombinant human bone morphogenetic protein-2 (BMP2) was purchased from R&D systems.

Reverse transcriptase-PCR (RT-PCR) and quantitative real-time RT-PCR analysis

Total RNAs were extracted from differentiated and undifferentiated CL6 cells and mouse embryonic stem (ES) cells with RNeasy minikit and DNase I treatment (QIAGEN). Mouse ES cell (129 strains) RNA, mouse heart total RNA (Clontech) and mouse skeletal muscle/total RNA (UNITECH. Co., Ltd.) were used as a positive control for each primer. Total RNA (2.0 µg each) for RT-PCR was converted to cDNA with Superscript^{TM} III RNase H– reverse transcriptase (Invitrogen), according to the manufacturer's manual. PCR conditions were optimized and linear amplification range was determined for each primer by varying annealing temperature and cycle number. PCR products were identified by positive control size. RT-PCR was performed using the primers of the genes of cardiac specific transcription factors: *Csx/Nkx2.5*, *Gata4*, *Mef2c*, *Hand2*; circulating hormone: *ANP*, *BNP*; cardiac structural proteins: *β-MyHC*, *MyLC-2a*, *MyLC-2v*; cytokines: *Bmp2*, *Bmp4*, *Fgf8*, *Greml*, *Wnt1*, *Wnt3a*, *Wnt5a*, *Wnt7a*, *Wnt11*; smooth muscle structural protein: smooth muscle-myosin heavy chain (*SM-MyHC*); the early mesodermal marker: *BrachyuryT*, *T-box6* (*Tbx6*); and *Gapdh* as control. PCR was performed with exTaq DNA polymerase and exTaq PCR buffer (TaKaRa) or LATaq DNA polymerase and GC buffer I (TaKaRa) for 25 or 30 cycles, with each cycle consisting of 95°C for 30 s, 50°C, 55°C, 60°C or 65°C for 45 s, and 72°C for 45 s, with an additional 5 min incubation at 72°C after completion of the final cycle. PCR primers for the genes of *Csx/Nkx2.5*, *Gata4*, *Mef2c*, *Hand2*, *ANP*, *BNP*, *β-MyHC*, *MyLC-2a*, *MyLC-2v*, *Bmp2*, *Bmp4*, *Fgf8*, *Greml*, *Wnt1*, *Wnt3a*, *Wnt5a*, *Wnt7a*, *Wnt11*, *SM-MyHC*, *BrachyuryT*, *Tbx6*, and *Gapdh* (Table S1a) were obtained from Mouse Genome

Informatics (http://www.informatics.jax.org/). The PCR products were size-fractionated by 2% agarose gel electrophoresis.

Quantitative real-time RT-PCR was performed on an ABI Prism 7700 Sequence Detection System (Applied Biosystems), using 100 ng of cDNA in 25 µl reaction volume with 10 nmol/l of each primer, and 12.5 µl SYBR Green Realtime PCR Master Mix (TOYOBO). PCR primers for the genes of *Bmp2*, *Bmp4*, *Wnt3a*, and *Gapdh* (Table S1b) were obtained from PrimerBank (http://pga.mgh.harvard.edu/primerbank/index.html). Calculations were automatically performed by ABI software (Applied BioSystems).

Immunocytochemistry

A laser confocal microscope (LSM510, Zeiss) was used for immunocytochemical analysis. Differentiated and undifferentiated CL6 cells were fixed with 4% paraformaldehyde (Wako) for 5 min at 4°C and treated with 0.1% triton X-100 (Sigma) in PBS for 20 min at room temperature, then incubated for 20 min at room temperature in a protein-blocking solution consisting of PBS supplemented with 5% normal goat serum (DakoCytomation). These CL6 cells were then incubated overnight with primary antibody monoclonal anti-sarcomeric myosin antibody (MF20, mouse IgG_{2b} isotype, 1 mg/ml, University of Iowa Hybridoma Bank) and Troponin T, and Cardiac Isoform Ab-1 clone 13-11 (cTnT, mouse IgG_1 isotype, 1:300, Lab Vision Corp), or the monoclonal anti-α-actinin (SARCOMERIC) CLONE EA-53 (α-actinin, mouse IgG_1 isotype, 1:300, Sigma) in PBS at 4°C. The cells were extensively washed in PBS and incubated at room temperature with Alexa Fluor 568-conjugated goat anti-Mouse IgG_{2b} (anti-MF20) (Molecular Probe; diluted 1:300), Alexa Fluor 488-conjugated goat anti-mouse IgG_1 (anti-cTnT) (Molecular Probe; diluted 1:300), Alexa Fluor 546-conjugated goat anti-mouse IgG(H+L) (anti-α-actinin) (Molecular Probe; diluted 1:300), and nuclei were counterstained with 4′, 6-diamidino-2-phenylindole (DAPI) (Wako; diluted 1:300) for 45 min. To prevent fading, cells were then mounted in DakoCytomation Fluorescent Mounting Medium (DakoCytomation).

Transfection and luciferase assays

Cells (8.0×10^5) seeded and cultured in 60 mm dishes (Becton Dickinson) were transfected 18 h after plating using Lipofectamine 2000 (Invitrogen) and PLUS reagent (Invitrogen) in Opti-MEM (Gibco). Transfection contained 1.0 µg of TOPflash plasmid (Upstate Biotechnology) for measurement of Wnt/β-catenin activity, or 5.0 µg of the *Id1* promoter-Lux plasmid (provided by Dr Imamura and Dr Miyazono) for measurement of BMP-induced *Id1* gene transcription, and 0.5 µg of pRL-CMV (Promega) as co-transfected control. Medium containing 10% FBS was changed 3 h after transfection and transfected cells (1.8×10^5) were re-seeded in 6-well plates 24 h after transfection. After 18 h, CL6 cells were induced with BMP2 (100 ng/ml) and DMSO. CL6 cells were prepared for luciferase activity analysis using Dual luciferase reporter assay system (Promega).

Area calculation

The regions of interest (beating area, immunostaining area) were defined in Photoshop (Adobe systems) using the 'magic wand' tool. The total numbers of pixels identified were then counted using the histogram function. At least five different fields were measured for each dish.

Statistical analysis

Results, shown as the mean±SE, were compared by ANOVA followed by Scheffé's test, with $P<0.05$ considered significant.

Supporting Information

Figure S1 A semi-quantitative RT-PCR of cardiomyocyte-specific genes. To investigate expression level of cardiomyocyte-specific genes (Csx/Nkx2.5, Gata4, MyLC-2a, and MyLC-2v), a semi-quantitative RT-PCR was performed from CL6 cells treated with 1% DMSO and the indicated concentration of Grem1 for 14 days. Each RT-PCR product was electrophoresed in 2% agarose gel, and was measured using ImageJ software (http://rsb.info.nih.gov/ij/) to calculate the ratio of each gene to Gapdh. The expression level for each gene is determined relative to that of Gapdh, and expression level in CL6 cells treated with DMSO alone was regarded as 1.0. The relative expression levels were averaged from at least three independent experiments.

Found at: doi:10.1371/journal.pone.0002407.s001 (1.04 MB DOC)

Figure S2 Grem1 enhanced cardiomyogenic differentiation of mouse ES cells. Mouse ES cells (NCH1.5, C57BL/6J×129ter/Sv) were cultured on a mouse embryonic fibroblast feeder layer inactivated with 30 Gy γ-irradiation in gelatin-coated 60 mm dishes (Becton, Dickinson). Cells were grown in KnockOut DMEM (Gibco) supplemented with 15% fetal bovine serum (Cell Culture Technologies), 2 mM GlutaMAX (Gibco), 0.1 mM non-essential amino acid (Gibco), 0.1 mM 2-mercaptoethanol (Gibco), penicillin, streptomycin, and 2,000 U/ml mouse leukemia inhibitory factor (LIF) (Chemicon). For cardiomyogenic differentiation, ES cells were exposed to 125 ng/ml Grem1 (R&D systems) for the three days. The cells were then trypsinized and cultured to form embryonic bodies (EBs) from a single cell using a three-dimensional culture system (without LIF) on low cell binding dishes (96-well plate round bottom). This represented day 0 of EB formation. On the next day, the medium was replaced with the same medium without LIF. EBs were re-seeded on gelatin-coated 48-well plates with one EB per well, on day 8 after the start of EB formation. The cardiomyogenic induction was estimated by the beating EB number per total EB number, measured on day 12 under a phase-contrast microscope. Grem1 increased the percentage of beating EBs to 69.2%, as compared with 26.7% in EBs without Grem1 treatment. The numbers in parentheses indicate the EB numbers counted.

Found at: doi:10.1371/journal.pone.0002407.s002 (1.27 MB DOC)

Table S1 Primer sequences.

Found at: doi:10.1371/journal.pone.0002407.s003 (0.06 MB DOC)

Movie S1 CL6 cells treated with DMSO alone. P19CL6 cells are reproducibly and stably induced into beating cardiomyocytes with DMSO.

Found at: doi:10.1371/journal.pone.0002407.s004 (1.66 MB MOV)

Movie S2 CL6 cells treated with Grem1 (125 ng/ml) and DMSO. Grem1 dramatically promotes DMSO-induced cardiomyogenic differentiation of P19CL6 cells at a concentration of 125 ng/ml.

Found at: doi:10.1371/journal.pone.0002407.s005 (2.40 MB MOV)

Acknowledgments

We would like to express our sincere thanks to T. Imamura and K. Miyazono for the *Id1* promoter-Lux plasmid, and J. Fujimoto for their discussion of this work.

Author Contributions

Conceived and designed the experiments: AU DK. Performed the experiments: DK HM RI KM. Analyzed the data: AU AN DK YT RI MT MW. Contributed reagents/materials/analysis tools: IK AN IS HS. Wrote the paper: AU DK.

References

1. Andree B, Duprez D, Vorbusch B, Arnold HH, Brand T (1998) BMP-2 induces ectopic expression of cardiac lineage markers and interferes with somite formation in chicken embryos. Mech Dev 70: 119–131.
2. Schultheiss TM, Burch JB, Lassar AB (1997) A role for bone morphogenetic proteins in the induction of cardiac myogenesis. Genes Dev 11: 451–462.
3. Angello JC, Kaestner S, Welikson RE, Buskin JN, Hauschka SD (2006) BMP induction of cardiogenesis in P19 cells requires prior cell-cell interaction(s). Dev Dyn 235: 2122–2133.
4. Alsan BH, Schultheiss TM (2002) Regulation of avian cardiogenesis by Fgf8 signaling. Development 129: 1935–1943.
5. Crossley PH, Martin GR (1995) The mouse Fgf8 gene encodes a family of polypeptides and is expressed in regions that direct outgrowth and patterning in the developing embryo. Development 121: 439–451.
6. Reifers F, Walsh EC, Leger S, Stainier DY, Brand M (2000) Induction and differentiation of the zebrafish heart requires fibroblast growth factor 8 (fgf8/acerebellar). Development 127: 225–235.
7. Whitehead GG, Makino S, Lien CL, Keating MT (2005) fgf20 is essential for initiating zebrafish fin regeneration. Science 310: 1957–1960.
8. Yamagishi H, Olson EN, Srivastava D (2000) The basic helix-loop-helix transcription factor, dHAND, is required for vascular development. J Clin Invest 105: 261–270.
9. Ariizumi T, Kinoshita M, Yokota C, Takano K, Fukuda K, et al. (2003) Amphibian in vitro heart induction: a simple and reliable model for the study of vertebrate cardiac development. Int J Dev Biol 47: 405–410.
10. Gavert N, Ben-Ze'ev A (2007) beta-Catenin signaling in biological control and cancer. J Cell Biochem 102: 820–828.
11. Chien KR, Moretti A, Laugwitz KL (2004) Development. ES cells to the rescue. Science 306: 239–240.
12. Pandur P, Lasche M, Eisenberg LM, Kuhl M (2002) Wnt-11 activation of a non-canonical Wnt signalling pathway is required for cardiogenesis. Nature 418: 636–641.
13. Yamagishi H, Yamagishi C, Nakagawa O, Harvey RP, Olson EN, et al. (2001) The combinatorial activities of Nkx2.5 and dHAND are essential for cardiac ventricle formation. Dev Biol 239: 190–203.
14. Park M, Wu X, Golden K, Axelrod JD, Bodmer R (1996) The wingless signaling pathway is directly involved in Drosophila heart development. Dev Biol 177: 104–116.
15. Marvin MJ, Di Rocco G, Gardiner A, Bush SM, Lassar AB (2001) Inhibition of Wnt activity induces heart formation from posterior mesoderm. Genes Dev 15: 316–327.
16. Schneider VA, Mercola M (2001) Wnt antagonism initiates cardiogenesis in Xenopus laevis. Genes Dev 15: 304–315.
17. Tzahor E, Lassar AB (2001) Wnt signals from the neural tube block ectopic cardiogenesis. Genes Dev 15: 255–260.
18. Olson EN (2001) Development. The path to the heart and the road not taken. Science 291: 2327–2328.
19. Terami H, Hidaka K, Katsumata T, Iio A, Morisaki T (2004) Wnt11 facilitates embryonic stem cell differentiation to Nkx2.5-positive cardiomyocytes. Biochem Biophys Res Commun 325: 968–975.
20. Sharov AA, Dudekula DB, Ko MS (2005) A web-based tool for principal component and significance analysis of microarray data. Bioinformatics 21: 2548–2549.
21. Hamatani T, Carter MG, Sharov AA, Ko MS (2004) Dynamics of global gene expression changes during mouse preimplantation development. Dev Cell 6: 117–131.
22. Sharov AA, Dudekula DB, Ko MSH (2005) http://lgsun.grc.nia.nih.gov/ANOVA/help.html#hierarchical Accessed 2007 April 20. Bioinformatics Advance Access.
23. Naito AT, Akazawa H, Takano H, Minamino T, Nagai T, et al. (2005) Phosphatidylinositol 3-kinase-Akt pathway plays a critical role in early cardiomyogenesis by regulating canonical Wnt signaling. Circ Res 97: 144–151.
24. Hsu DR, Economides AN, Wang X, Eimon PM, Harland RM (1998) The Xenopus dorsalizing factor Gremlin identifies a novel family of secreted proteins that antagonize BMP activities. Mol Cell 1: 673–683.
25. Naito AT, Shiojima I, Akazawa H, Hidaka K, Morisaki T, et al. (2006) Developmental stage-specific biphasic roles of Wnt/beta-catenin signaling in cardiomyogenesis and hematopoiesis. Proc Natl Acad Sci U S A 103: 19812–19817.
26. Jin EJ, Erickson CA, Takada S, Burrus LW (2001) Wnt and BMP signaling govern lineage segregation of melanocytes in the avian embryo. Dev Biol 233: 22–37.
27. Sutherland MK, Geoghegan JC, Yu C, Turcott E, Skonier JE, et al. (2004) Sclerostin promotes the apoptosis of human osteoblastic cells: a novel regulation of bone formation. Bone 35: 828–835.
28. Shi W, Zhao J, Anderson KD, Warburton D (2001) Gremlin negatively modulates BMP-4 induction of embryonic mouse lung branching morphogenesis. Am J Physiol Lung Cell Mol Physiol 280: L1030–1039.
29. Tzahor E, Kempf H, Mootoosamy RC, Poon AC, Abzhanov A, et al. (2003) Antagonists of Wnt and BMP signaling promote the formation of vertebrate head muscle. Genes Dev 17: 3087–3099.
30. Zuniga A, Michos O, Spitz F, Haramis AP, Panman L, et al. (2004) Mouse limb deformity mutations disrupt a global control region within the large regulatory landscape required for Gremlin expression. Genes Dev 18: 1553–1564.
31. Michos O, Panman L, Vintersten K, Beier K, Zeller R, et al. (2004) Gremlin-mediated BMP antagonism induces the epithelial-mesenchymal feedback signaling controlling metanephric kidney and limb organogenesis. Development 131: 3401–3410.
32. Yuasa S, Itabashi Y, Koshimizu U, Tanaka T, Sugimura K, et al. (2005) Transient inhibition of BMP signaling by Noggin induces cardiomyocyte differentiation of mouse embryonic stem cells. Nat Biotechnol 23: 607–611.
33. Singh JP, Chaikin MA, Pledger WJ, Scher CD, Stiles CD (1983) Persistence of the mitogenic response to platelet-derived growth factor (competence) does not reflect a long-term interaction between the growth factor and the target cell. J Cell Biol 96: 1497–1502.
34. Frank NY, Kho AT, Schatton T, Murphy GF, Molloy MJ, et al. (2006) Regulation of myogenic progenitor proliferation in human fetal skeletal muscle by BMP4 and its antagonist Gremlin. J Cell Biol 175: 99–110.
35. Klaus A, Saga Y, Taketo MM, Tzahor E, Birchmeier W (2007) Distinct roles of Wnt/beta-catenin and Bmp signaling during early cardiogenesis. Proc Natl Acad Sci U S A 104: 18531–18536.
36. Yamaguchi TP, Takada S, Yoshikawa Y, Wu N, McMahon AP (1999) T (Brachyury) is a direct target of Wnt3a during paraxial mesoderm specification. Genes Dev 13: 3185–3190.
37. Kleber M, Lee HY, Wurdak H, Buchstaller J, Riccomagno MM, et al. (2005) Neural crest stem cell maintenance by combinatorial Wnt and BMP signaling. J Cell Biol 169: 309–320.
38. Sugiki T, Uyama T, Toyoda M, Morioka H, Kume S, et al. (2007) Hyaline cartilage formation and enchondral ossification modeled with KUM5 and OP9 chondroblasts. J Cell Biochem 100: 1240–1254.

MOLECULAR AND CELLULAR BIOLOGY, Apr. 2008, p. 2125–2137 Vol. 28, No. 7
0270-7306/08/$08.00+0 doi:10.1128/MCB.00740-07
Copyright © 2008, American Society for Microbiology. All Rights Reserved.

Inducible Expression of Chimeric EWS/ETS Proteins Confers Ewing's Family Tumor-Like Phenotypes to Human Mesenchymal Progenitor Cells[▽]†

Yoshitaka Miyagawa,[1] Hajime Okita,[1]* Hideki Nakaijima,[1] Yasuomi Horiuchi,[1] Ban Sato,[1] Tomoko Taguchi,[1] Masashi Toyoda,[3] Yohko U. Katagiri,[1] Junichiro Fujimoto,[2] Jun-ichi Hata,[1] Akihiro Umezawa,[3] and Nobutaka Kiyokawa[1]

Department of Developmental Biology, National Research Institute for Child Health and Development, 2-10-1, Okura, Setagaya-ku, Tokyo 157-8535, Japan[1]; National Research Institute for Child Health and Development, 2-10-1, Okura, Setagaya-ku, Tokyo 157-8535, Japan[2]; and Department of Reproductive Biology, National Research Institute for Child Health and Development, 2-10-1, Okura, Setagaya-ku, Tokyo 157-8535, Japan[3]

Received 27 April 2007/Returned for modification 13 July 2007/Accepted 7 January 2008

Ewing's family tumor (EFT) is a rare pediatric tumor of unclear origin that occurs in bone and soft tissue. Specific chromosomal translocations found in EFT cause EWS to fuse to a subset of ets transcription factor genes (ETS), generating chimeric EWS/ETS proteins. These proteins are believed to play a crucial role in the onset and progression of EFT. However, the mechanisms responsible for the EWS/ETS-mediated onset remain unclear. Here we report the establishment of a tetracycline-controlled EWS/ETS-inducible system in human bone marrow-derived mesenchymal progenitor cells (MPCs). Ectopic expression of both EWS/FLI1 and EWS/ERG proteins resulted in a dramatic change of morphology, i.e., from a mesenchymal spindle shape to a small round-to-polygonal cell, one of the characteristics of EFT. EWS/ETS also induced immunophenotypic changes in MPCs, including the disappearance of the mesenchyme-positive markers CD10 and CD13 and the up-regulation of the EFT-positive markers CD54, CD99, CD117, and CD271. Furthermore, a prominent shift from the gene expression profile of MPCs to that of EFT was observed in the presence of EWS/ETS. Together with the observation that EWS/ETS enhances the ability of cells to invade Matrigel, these results suggest that EWS/ETS proteins contribute to alterations of cellular features and confer an EFT-like phenotype to human MPCs.

Ewing's family tumor (EFT) is a rare childhood cancer arising mainly in bone and soft tissue. Since EFT has a poor prognosis, it is important to elucidate the underlying pathogenic mechanisms for establishing a more effective therapeutic strategy. EFT is characterized by the presence of chimeric genes composed of EWS and ets transcription factor genes (ETS) formed by specific chromosomal translocations, i.e., EWS/FLI1, t(11;22)(q24;q12); EWS/ERG, t(21;22)(q12;q12); EWS/ETV1, t(7;22)(p22;q12); EWS/E1AF, t(17;22)(q12;q12); and EWS/FEV, t(2;22)(q33;q12) (26). The products of these chimeric genes behave as aberrant transcriptional regulators and are believed to play a crucial role in the onset and progression of EFT (3, 36). Indeed, recent studies have revealed that the induction of EWS/FLI1 proteins can trigger transformation in certain cell types, including NIH 3T3 cells (36), C2C12 myoblasts (12), and murine primary bone marrow-derived mesenchymal progenitor cells (MPCs) (6, 45, 52). However, studies have also indicated that overexpression of EWS/FLI1 provokes apoptosis and growth arrest in mouse normal embryonic fibroblasts and primary human fibroblasts (10, 31), hence hampering understanding of the precise role of EWS/ETS proteins in the development of EFT. The function of EWS/ETS proteins would be greatly influenced by cell type, and thus the cells that can originate EFTs might be more susceptible to the tumorigenic effects of EWS/ETS.

Although the cell origin of EFT is still unknown, the expression of neuronal markers in spite of the occurrence in bone and soft tissues has kept open the debate as to a potential mesenchymal or neuroectodermal origin. As described above, ectopic expression of EWS/FLI1 results in dramatic changes in morphology and the formation of EFT-like tumors in murine primary bone marrow-derived MPCs but not in murine embryonic stem cells (6, 45, 52), supporting the notion that MPCs are a plausible cell origin of EFT (45). However, others argue that MPCs cannot be considered progenitors of EFT without further evidence of similarity between human EFT and MPC-EWS/FLI1-induced tumors in mice (29, 46).

The development of experimental systems using murine species is useful for elucidating the mechanisms behind the pathogenesis of EFT. However, several differences between human and murine systems cannot be ignored; these differences include the expression patterns of surface antigens in MPCs, for instance (7, 44, 51, 53). Moreover, human cells are difficult to transform in vitro, and the transformed cells of mice seem to produce a more aggressive tumor than those of hu-

* Corresponding author. Mailing address: Department of Developmental Biology, National Research Institute for Child Health and Development, 2-10-1, Okura, Setagaya-ku, Tokyo 157-8535, Japan. Phone: 81-3-3416-0181. Fax: 81-3-3417-2496. E-mail: okita@nch.go.jp.

† Supplemental material for this article may be found at http://mcb.asm.org/.

▽ Published ahead of print on 22 January 2008.

Downloaded from mcb.asm.org at Keio University Shinanomachi Media Center on July 10, 2008